eLife

Reviewed Preprint
v1 • September 26, 2025
Not revised

Reviewed Preprint
v2 • May 11, 2026
Revised by authors

For correspondence:
eparesp@gmail.com

Competing interests: No competing interests declared

Funding: See page 34

Reviewing editor: Tobias H Donner, University Medical Center Hamburg-Eppendorf, Germany

Perceptual glimpses are locally accumulated and globally maintained at distinct processing levels

Elisabeth Parés-Pujolràs[1], Anna C Geuzebroek[1], Redmond G O'Connell[2], Simon P Kelly[1]

[1]School of Electrical and Electronic Engineering and UCD Centre for Biomedical Engineering, University College Dublin, Dublin, Ireland • [2]Trinity College Institute of Neuroscience and School of Psychology, Trinity College Dublin, Dublin, Ireland

eLife Assessment

This study presents **valuable** findings on the physiological and computational underpinnings of the accumulation of intermittent glimpses of sensory evidence. The evidence supporting the claims of the authors is **solid**, although a more exhaustive characterisation of how the different signals interact would have strengthened the study. The work will be of interest to cognitive and systems neuroscientists working on decision-making.

https://doi.org/10.7554/eLife.107980.2.sa3

Abstract

Making decisions often requires the integration of multiple pieces of information. An extensive body of research has investigated the neural architecture underpinning evidence accumulation in perceptual tasks where information is continuously present, but less is known about how this neural architecture operates in situations affording only intermittent glimpses of an evidence source. In two electroencephalography (EEG) experiments, participants judged the direction of up to two pulses of motion evidence separated by gaps of varying duration. Our behavioural analysis found that participants used both pulses but underutilised the second, and showed no systematic decrease in accuracy as a function of gap duration. At the neural level, motor beta lateralisation tracked cumulative evidence across pulses, maintaining a sustained representation of the decision variable through the gap and until response. In contrast, the centroparietal positivity (CPP), a previously-characterised signature of evidence accumulation, built up transiently to a peak that scaled with each pulse's contribution to the decision variable (i.e. the absolute belief update it produced), falling back to baseline in between pulses. These patterns were recapitulated in a model where pulse-information transiently integrated at the CPP level is fed to and maintained at a bounded motor level, so that information presented later on in a trial is integrated only if a bound has not yet been reached.

1. Introduction

Perceptual decision-making is widely thought to involve a process of evidence integration over time (Hyafil et al., 2023). An extensive body of research has successfully linked these integration computations to multiple neural decision signals in various species (Gold & Shadlen, 2007; Hanks & Summerfield, 2017; Heekeren et al., 2008; O'Connell & Kelly, 2021; Shadlen & Kiani, 2013) revealing a neural decision architecture that includes both effector-selective motor preparation signals, and motor-independent signals that appear to reflect integration operations at an intermediate processing level (Gherman et al., 2024; O'Connell & Kelly, 2021; Okazawa & Kiani, 2023; Stockart et al., 2025). Such neural decision processes have mainly been studied in the context of tasks requiring immediate judgements about a single continuously-presented

stimulus. However, in many real-life situations a decision-maker is afforded only a short glimpse of a relevant evidence source and it is uncertain whether and when they will receive an additional glimpse, as, for example, when evaluating an object among moving traffic that may be intermittently occluded. This scenario has begun to be studied using an intermittent-evidence task (Kiani et al., 2013), which we refer to as "gaps task", in which up to two short pulses of noisy evidence for a certain motion direction are presented separated by a variable temporal gap, with a behavioural response required after a delayed cue. Previous studies using this task or variants of it have found that both evidence pulses are utilised, but not fully or equally (Azizi & Ebrahimpour, 2023; Golmohamadian et al., 2025; Kiani et al., 2013; Tohidi-Moghaddam et al., 2019), and although a general information leakage account could be ruled out based on the absence of any decline in accuracy with gap duration, the neural underpinnings of the task, including the functional roles of effector-selective and motor-independent processes in handling and maintaining the intermittent evidence, and how such information underutilisation can arise, have remained unclear.

In humans, two neurophysiological signatures of decision formation can be utilised alongside behavioural data to gain insight into mechanisms underlying perceptual tasks (O'Connell & Kelly, 2021). First, spectral activity in the beta band (13-30 Hz), long observed to decrease over motor cortex with preparation of a contralateral limb (Pfurtscheller & Lopes da Silva, 1999; Stancák & Pfurtscheller, 1995), has been found in decision tasks to build at an evidence-dependent rate, reaching a threshold level contralateral to, and coincident with, the executed action (Donner et al., 2009; Feuerriegel et al., 2021; Geuzebroek et al., 2023; Kelly et al., 2021; O'Connell et al., 2012; Steinemann et al., 2018). Motor beta dynamics have also been shown to reflect decisions and choice biases in humans (de Lange et al., 2013; Gould et al., 2012; Herding et al., 2016; Pape & Siegel, 2016; Urai & Donner, 2022; Wyart et al., 2015) and non-human primates (Haegens et al., 2011, 2017; Rassi et al., 2023), highlighting its role as a key marker of decision-related activity. Second, a centroparietal positivity (CPP) in the human electroencephalogram (EEG) has been found to exhibit similar evidence-dependent buildup dynamics in conventional perceptual tasks with continuous stimuli such as random dot motion, but with an earlier latency; it begins building at a stimulus-aligned onset time, rises at a rate that scales with evidence strength, and peaks at the time of action choice when immediate execution is allowed (Kelly & O'Connell, 2013; O'Connell et al., 2012; Steinemann et al., 2018). Signals with similar dynamics have been observed in multiple brain regions including the parietal cortex intracranial recordings (Gherman et al., 2024; Pereira et al., 2021; Stockart et al., 2025), bearing some overlap with regions identified in functional imaging studies (Liu & Pleskac, 2011; Ploran et al., 2007; Tremel & Wheeler, 2015). In contrast with motor preparation signals, the CPP exhibits evidence-integration dynamics even when no motor output is required (O'Connell et al., 2012). In delayed-response tasks where actions are deferred until some time after the perceptual choice is made, the CPP peaks at decision commitment and falls back to its baseline level (Azizi & Ebrahimpour, 2023; McCone et al., 2026; Twomey et al., 2016), whereas relative motor preparation reflected in motor beta lateralisation (MBL) sustains until action execution (Donner et al., 2009; McCone et al., 2026; Murphy et al., 2021; Parés-Pujolràs et al., 2025; Twomey et al., 2016). These findings are consistent with the CPP tracking an intermediary, motor-independent evidence integration process that is continuously fed to downstream motor preparation, where a sustained representation of the DV is maintained after commitment is reached, until a response is made.

More recently, a few studies have highlighted that the CPP can behave differently in expanded judgement tasks, where evidence is presented as a series of discrete tokens that need to be integrated rather than as a continuous, noisy stream. In these tasks, centroparietal signals exhibit transient token-evoked positivities that scale with the immediate evidence, rather than tracking the evolution of an ongoing decision variable (DV) across tokens (Murphy et al., 2021; Parés-Pujolràs et al., 2025). Motor Beta Lateralisation (MBL), meanwhile, tracks the evolving decision variable across discrete tokens over multiple seconds, by stepping up or down according to the evidence in each token and sustaining in between them (Murphy et al., 2021; Parés-Pujolràs et

al., 2025; Wilming et al., 2020). These findings again point to the operation of an intermediary decision process reflected in the CPP - one that can be flexibly configured to compute different quantities depending on the nature of the task.

The Gaps task, like expanded judgment tasks, involves temporally disparate pieces of information, but it holds key distinctions that demand dedicated investigation. In expanded judgement tasks, tokens typically bear little or no perceptual noise, but the overlap of the underlying generative distributions means they often provide conflicting information (e.g. Balsdon et al., 2020, 2021; Glickman et al., 2022; Rouault et al., 2022; Waskom & Kiani, 2018; Wyart et al., 2015). The nature of the stimuli thus encourages appraisal of each token as a distinct object, potentially explaining the transient pattern of CPP activity. In contrast, the Gaps task involves pulses of evidence that are perceptually noisy but always indicate a consistent motion direction (Kiani et al., 2013), thus appearing as glimpses of the same object rather than a series of individual objects. Only one study has examined neural signatures of decision formation in this intermittent evidence context: using EEG, Azizi & Ebrahimpour (2023) showed that the CPP exhibits an evoked positivity after each pulse that appears to decay during the gap, suggesting a local processing role. However, how these pulse-evoked activities relate to the computations underpinning an ongoing decision, interact with motor preparation to determine choice, and relate to any information underutilisation, has not been examined.

In this study, we recorded EEG during the Gaps task (Kiani et al., 2013) in two experiments with slightly different settings for the variable temporal gaps to ensure generality of findings. Our primary goal was to characterise the dynamics of the CPP and MBL in the context of this intermittent evidence task, and functionally relate them to behavioural indices of integration across tokens. We found that participants based their choices on both pulses but with a weaker influence of pulse 2, and coherence-dependent weightings on choice were mirrored in the magnitude of transient pulse-evoked CPPs. These patterns could be explained by a decision architecture where the CPP conducts two separate rounds of evidence accumulation, continuously feeding the accumulating evidence within each pulse to a downstream motor process indexed by MBL. MBL in turn tracks a continuous representation of the state of the overall DV, sustaining without loss of information throughout the gap and between the final evidence and the response. Our behavioural and modelling results indicated that participants engaged in a bounded accumulation process, so that evidence samples within each pulse were only integrated while the DV encoded in MBL had not yet reached the bound. Additionally, given the dynamic structure of the task involving evidence onsets and offsets, we explored the dynamics of attention, as indexed by occipital alpha signals, and these were suggestive of a key role in filtering-out of irrelevant dot-motion, and in modulating the weight of pulses on choice.

2. Results

2.1. Behavioural results

In this study, participants engaged in a motion direction discrimination task where, on most trials, two pulses of partially-coherent dot motion (indicated by yellow dot colour) were separated by variable temporal 'gaps' in which motion was random, and thus uninformative (indicated by blue dot colour; Fig. 1A). Though coherence could differ, the direction was always consistent between the two pulses, so that they would be construed as two glimpses of the same evidence source. Our two experiments (Exp. 1: N = 22; Exp. 2: N = 21) differed only in the delays separating the two pulses. In both experiments, coherence levels were titrated for each participant using a staircase procedure aiming for an average 70% accuracy following a single evidence pulse. High (Exp. 1: M = 44.73%, SD = 12.64%; Exp 2: M = 33.04%, SD = 13.41%) and low (Exp. 1: M = 26.75%, SD = 7.74%; Exp 2: M =19.82%, SD = 8.04%) coherences were then set to be, respectively, 25% higher and 25% lower than the staircase-estimated coherence (see *Methods*), and small adjustments were made between blocks if performance substantially changed (*Figure S1*).

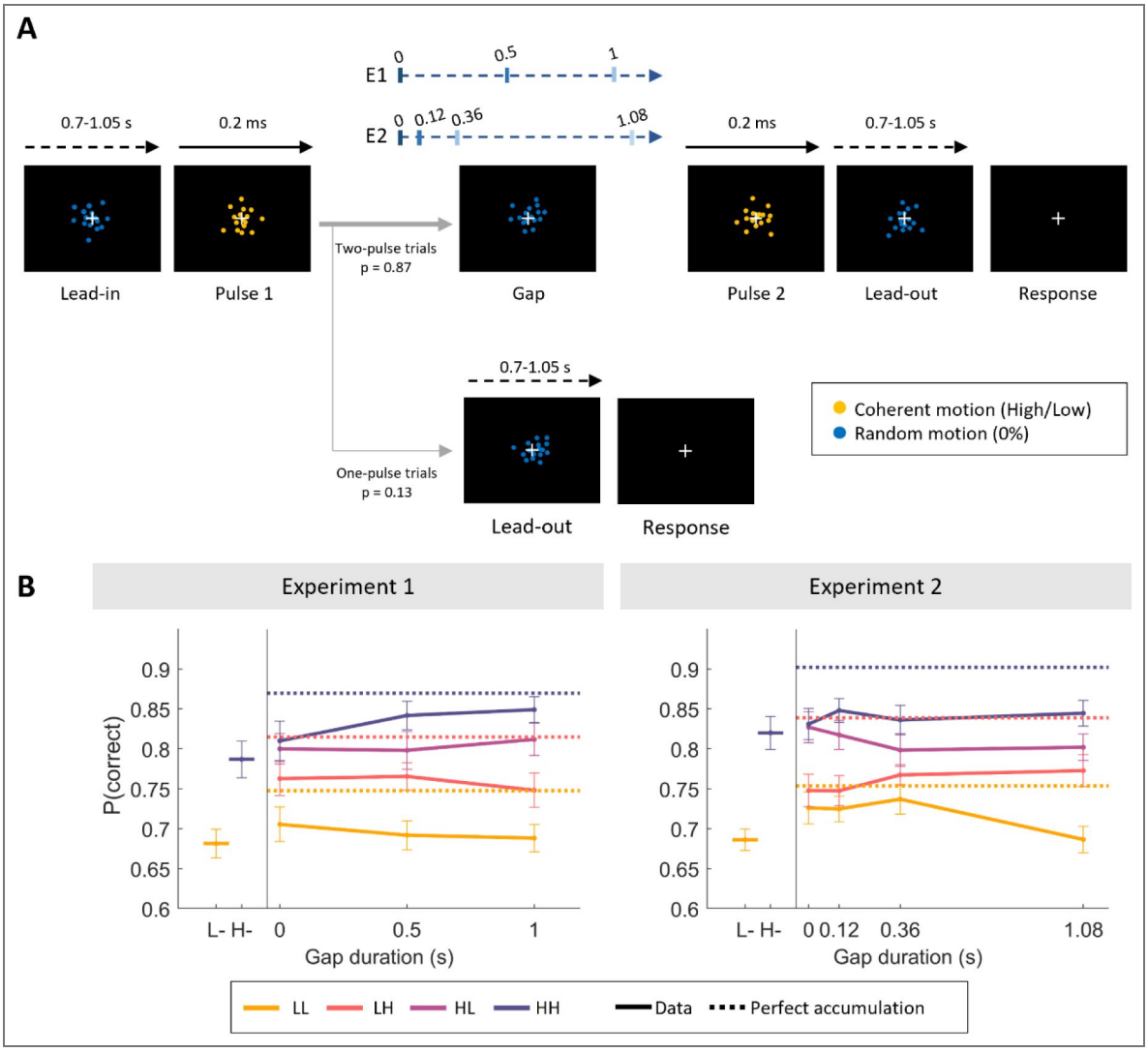

Figure 1. Task and behavioural results.

A. Experimental structure. Participants viewed a random dot stimulus that coherently moved either to the left or right during yellow evidence pulses, of which there was sometimes one, but usually two, separated by a variable gap in evidence indicated by blue dot colour. **B.** Grand-averaged (mean ± SEM) accuracy in two-pulse trials, sorted by pulse coherence (low, L/ high, H), order (LL, LH, HL, HH) and gap duration. Data points in the left-hand section indicate single-pulse accuracies. Overlaid horizontal dashed lines indicate the expected accuracy of a perfect accumulator, based on the grand-average performance on one-pulse trials. Note that a perfect accumulator predicts identical accuracies for the HL and LH conditions, and therefore the two lines overlap.

As expected, participants' accuracy scaled with motion coherence and number of pulses. In one-pulse trials, participants were more accurate in the high coherence compared to the low coherence trials (*Eq. 1*, Exp 1: β_1 = 0.33 ± 0.05, p < 0.001; Exp 2: β_1 = 0.43 ± 0.06, p < 0.001, Figure 1A). There was a further benefit in accuracy from the second pulse when present, indicated by sensitivity to coherence in both the first (*Eq.2*, Exp 1: β_1 = 0.26 ± 0.06, p < 0.001; Exp 2: β_1 = 0.31 ± 0.05, p < 0.001) and second (*Eq.2*, Exp 1: β_2 = 0.16 ± 0.06, p = 0.001; Exp 2: β_2 = 0.06 ± 0.04, p = 0.015) pulses. When both pulses in a two-pulse trial were the same coherence, participants performed better compared to one-pulse trials, exhibited both in high and low coherence trials in Experiment 2 (*Eq. 3*, Exp. 2: β_1 = 0.16 ± 0.08, p = 0.047; β_3 = 0.02 ± 0.08, p = 0.784), but only significantly so in high coherence trials in Experiment 1 (*Eq. 3*, Exp. 1: β_1 = 0.21 ± 0.07, p = 0.013; β_3 = 0.16 ± 0.07, p = 0.019). However, they did not perform as well as expected from a perfect accumulator (Figure 1B), estimated using performance in one-pulse trials to predict expected accuracy in two-pulse ones (see *Eq.* 5-7; see *Methods*).

The fact that the regression coefficients for the second pulse were smaller than those estimated for the first one indicates that participants' choices were guided more strongly by the first piece of evidence they received. On average, accuracies were lowest for the most difficult trials (both pulses had low motion coherence, LL), intermediate for trials with mixed coherences (LH, HL) and highest for the easiest trials (both pulses had high motion coherence, HH). However, we also observed a significant pulse-order effect: when the two presented pulses had different coherences, participants were more accurate when the first pulse was the high-coherence one (HL) compared to trials where the first pulse was low-coherence (LH) in both experiments (*Eq. 4*, Exp 1: β_2 = -0.11 ± 0.03, p <0.001; Exp 2: β_2 = -0.12 ± 0.02, p <0.001; Figure 1B). This is in line with participants' choices being more strongly influenced by the first evidence pulse.

Importantly, there was no main effect of gap duration on accuracies (*Eq. 2*, Exp 1: β_3 = 0.06 ± 0.08, p =0.525; Exp 2: β_3 = -0.003 ± 0.05, p =0.579; Figure 1B), suggesting an absence of leakage of information from the first pulse, in line with previous work (Azizi & Ebrahimpour, 2023; Kiani et al., 2013). However, in Experiment 2, gap duration interacted with the coherence of the second pulse (*Eq 2*, Exp 2: β_5 (p2 x gap interaction) = 0.16 ± 0.07, p =0.031). Since this effect was inconsistent across experiments and we did not have prior hypotheses about it, we leave it to one side and focus on the main effects of coherence. In what follows, we combine EEG and computational modelling to test the possibility that the greater sensitivity to the first pulse arises from the participants engaging in a bounded accumulation process where decisions are sometimes terminated early, curtailing the extent to which the second pulse benefits accuracy and driving the coherence order effects.

2.2. EEG results

2.2.1. Activity during the gap

We then turned to neural correlates of evidence accumulation during the task, specifically, MBL and the CPP. Across the two experiments and in all gap conditions, MBL showed evidence-dependent buildup continuously through the sequence of pulses with a temporal lag (Fig. 2A), sustaining at a coherence-dependent level (see Fig. S2; S3) throughout the gap between the two pulses and until response, showing stronger lateralisation towards the correct response following high-coherence pulses. In contrast, the CPP exhibited a transient build-up following each evidence pulse, falling back to baseline levels prior to the second pulse (Fig. 2B).

Given that our task included strong external (colour) cues indicating time windows with and without evidence, we further investigated the dynamics of attentional engagement with the stimulus, as indexed by occipital alpha activity (Foxe & Snyder, 2011; Van Diepen et al., 2019), throughout trial time. In both experiments, we observed strong occipital alpha desynchronisation (i.e. a decrease relative to baseline) during the periods in which the CPP indicated active evaluation of the yellow-dot evidence periods (Fig. 2C), and strongly elevated alpha above baseline levels in between those pulse-processing periods. Adding to the above behavioural finding of no main effect of gap duration, this suggests that the participants successfully gated

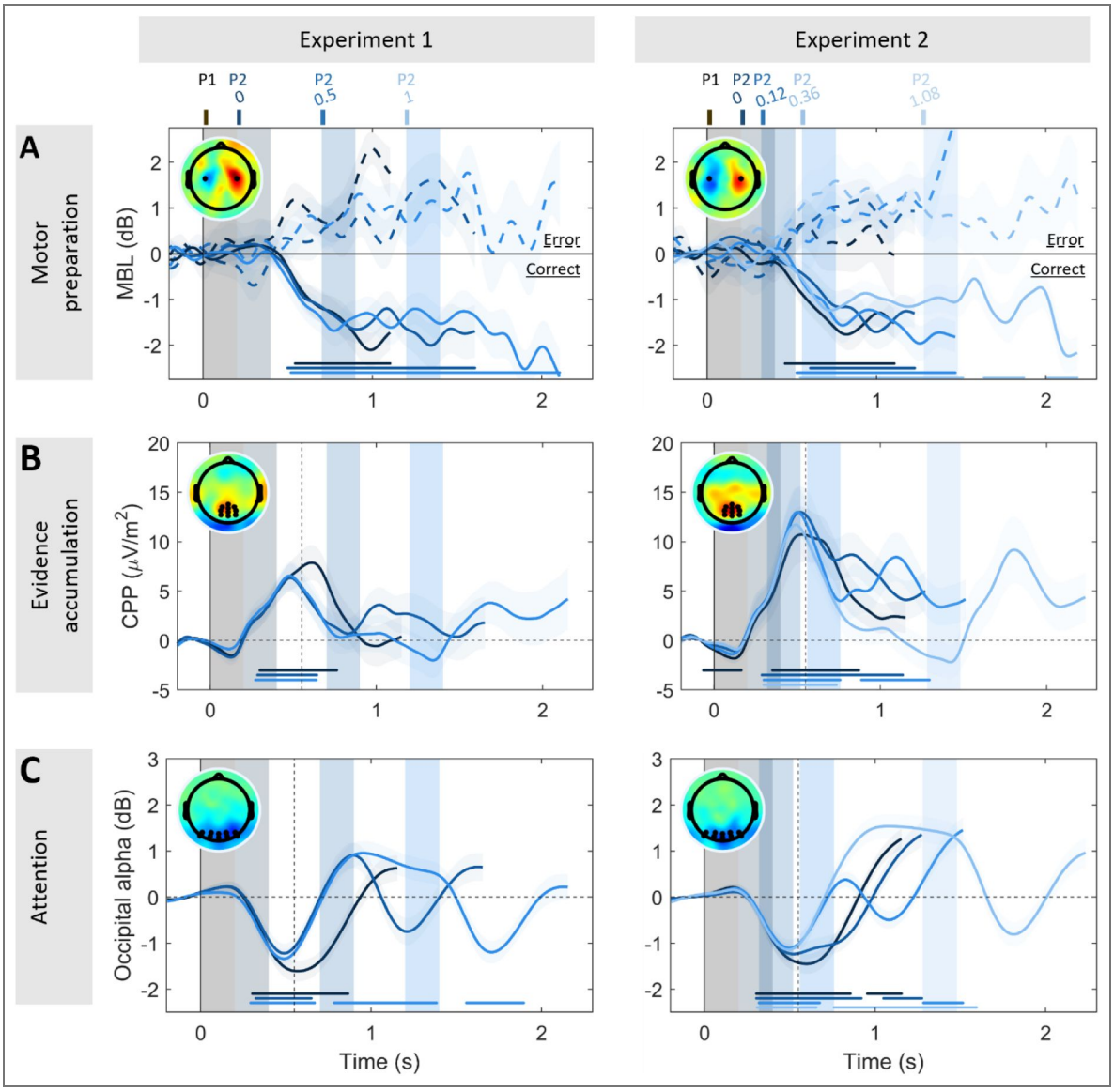

Figure 2. Neural correlates of evidence accumulation and motor preparation across temporal gaps.

A. Grand-averaged (±SEM) motor beta lateralisation (MBL) [Contra-Ipsilateral hemispheres with respect to correct response hand], sorted by accuracy (*solid line* correct, *dashed line* error). Participants started preparing a motor response in response to the first pulse, and MBL was sustained throughout the gap and until the time of behavioural response across all gap conditions in both experiments. **B.** Grand-averaged (±SEM) centroparietal positivity (CPP) across all temporal gap conditions. The CPP showed transient evoked responses following each pulse. Note that the evoked amplitudes by P1 (CPP-P1) were systematically higher than those evoked by P2 (CPP-P2) (Exp. 1: CPP-P2 = 52% of CPP-P1 peak amplitude; Exp. 2: CPP-P2 = 58% of CPP-P1 peak amplitude; see also Fig. S8). **C.** Grand-averaged (±SEM) occipital alpha power for each of the gap conditions, baseline-corrected before the onset of the first pulse and collapsed across coherence. Occipital alpha power showed a steep decrease following pulse onset (which was clearly indicated by a change in the colour of the moving dots), and steep increase overshooting the baseline level once the dots changed colour again to indicate non-coherent motion. Note that for both motor beta and alpha, greater negative values reflect greater preparation of the correct response and attention, respectively. In all panels, shaded areas indicate the timing of evidence pulses for the various gap durations, which are colour coded (see top axis). Topographies illustrate MBL before response (right minus left responses, ***A***) in correct trials, and CPP/alpha power 550 ms post stimulus onset (*dashed line, **B,C***). Further, markers along the bottom indicate times where the signal significantly differed from zero (two-tailed cluster-based permutation test, p<0.005) in only correct trials for MBL for consistency of polarity (***A***), and for all trials pooled in the case of the CPP (***B***) and alpha (***C***). Note that evidence-dependent buildup dynamics are clearly delayed in MBL relative to the CPP, and this aligns with previous research supporting the contention that the CPP lies upstream from motor preparation (Steinemann et al. 2018); such time delays were not a focus of the present study because in such delayed-response conditions we do not have access to the time of decision commitment.

stimulus evaluation according to dot colour, selectively attending to the temporal windows in which decision-relevant information is available for evaluation, and ignoring the decision-irrelevant gap periods.

2.2.2. Centroparietal signals transiently reflect local accumulation of evidence in each pulse

Next, we examined coherence-dependent CPP dynamics during the pulses. The CPP evoked after the first pulse (CPP-P1) scaled with the strength of evidence as expected, building more steeply (Exp. 1: $t_{(21)} = 2.18$, $p = 0.04$; Exp. 2: $t_{(20)} = 3.48$, $p = 0.002$) and reaching higher amplitudes after high coherence pulses compared to low-coherence ones over a cluster of centroparietal electrodes (Exp. 1: $p = 0.009$, Exp. 2: $p = 0.031$; two-tailed cluster-based permutation test; Fig. 3A-D). Furthermore, single-trial variability in CPP-P1 amplitude significantly modulated the first pulse's weight on choice: in trials where evoked CPP-P1 amplitudes were particularly high, the coherence of pulse 1 had a stronger influence on behaviour (Fig. S11A).

The coherence of the second pulse modulated peak amplitude in the standard way, with larger CPP amplitudes in trials with high pulse 2 coherence, although this effect was only significant in Experiment 2 (Exp. 1: $p = 0.165$, Exp.2: $p = 0.009$; two-tailed cluster-based permutation test; Fig. 3F,H;). CPP-P2 amplitude was also influenced by the coherence of Pulse 1: on trials where the first pulse was low coherence, CPPs evoked by the second pulse reached higher amplitudes (Exp. 1: $p = 0.018$, Exp. 2: $p = 0.005$; two-tailed cluster-based permutation test; see Fig. 3F,H). Additionally, CPP-P2 amplitude was generally smaller than CPP-P1 amplitude, which was the case whether we computed CPP-P2 amplitudes after baseline-correction before pulse 2 onset (Exp. 1: $t(21) = 2.29$, $p = 0.032$; Exp. 2: $t(20) = 4.19$, $p < 0.001$) or after correction for CPP-P1 overlap (Exp. 1: $t(21) = 1.93$, $p = 0.067$; Exp. 2: $t(20) = 3.25$, $p = 0.003$; see *Methods* for details).

2.2.4. A single bounded decision process can account for key behavioural and neural patterns

We then aimed to identify a computational model that could account for the key behavioural accuracy and CPP amplitude effects observed in our data. Similar to previous studies (Azizi & Ebrahimpour, 2023; Kiani et al., 2013; Tohidi-Moghaddam et al., 2019) there was no evidence of leak in our data, given that no general decrease in accuracy was observed for longer gap durations. This lack of a main effect of gap duration on accuracies also indicates that participants did not accumulate the incoherent motion presented during the gaps. Instead, the primacy effect observed in our behavioural results, with higher accuracies in HL than LH trials, is consistent with a bounded process where participants sometimes terminated evidence accumulation early, failing to use all available evidence. Thus, we fitted a single bounded accumulator model with three free parameters (bound, high- and low-coherence drift rates), where evidence accumulation without leak proceeds only during the pulse time windows and is terminated upon bound crossing (see *Methods* for full details). The overall DV was sustained at the value attained at the end of pulse 1 throughout the gap. If the bound was not crossed by the end of the trial, the sign of the DV at the end of the trial determined the model's predicted choice.

This simple single-DV model could account for the order effects observed in behavioural data, where the first pulse had a greater bearing on choice than the second one, while at the same time capturing the generally greater accuracy of two-pulse trials compared to single-pulse ones (Fig. 4A). In this model, this partial benefit of the second pulse arises from the fact that the DV is further influenced by it only on the trials where the DV has not already reached a bound. The second pulse can thus be integrated to varying extents along a continuum: not at all (if a bound is hit during pulse 1), partially (if no bound was hit during pulse 1, and only until a bound is hit during pulse 2), or fully (if no bound is hit at any point during the trial). As expected, a greater proportion of trials terminate early in the P1-high trials compared to P1-low trials (Fig. 4B). Note that this simple diffusion model has no way to produce systematic gap-dependent effects, meaning that predicted accuracies are forced to be flat across gap durations; again, since the observed gap-dependent effects were unexpected and differed in our two experiments, we did not pursue

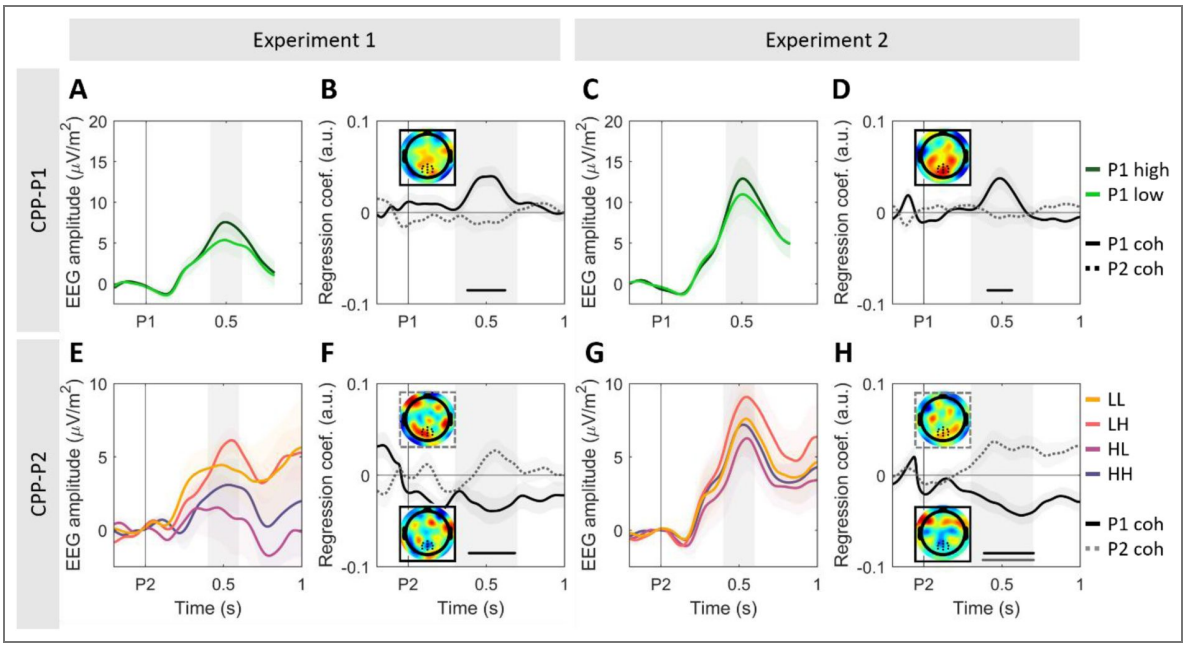

Figure 3. CPP amplitude following each pulse scales with its coherence, and the strength of evidence in pulse 1 additionally inversely modulates amplitudes following pulse 2.

A,C. Grand-averaged (±SEM) centroparietal activity after pulse 1 (CPP-P1), averaged across all gap conditions. **B,D.** Standardized regression coefficients illustrating the effect of P1 (*solid line*) and P2 (*dashed line*) coherence on evoked CPP-P1 amplitudes. Inset topographies illustrate the coherence effect [P1 high – P1 low] at [0.4-0.6s] after P1. **E,G.** Grand-averaged (±SEM) centroparietal activity after pulse 2 (CPP-P2), averaged over all non-zero gaps in the two experiments. For illustration purposes, we subtracted the average activity of long gap trials with the same P1 coherence from the epoched EEG traces, between [-0.2 to 1.4s] from P1 presentation, and baseline corrected traces [-100 to 0ms] before P2. This isolates the neural activity uniquely associated with the presentation of the second pulse in short gap trials (<1s), where potentials evoked by the first and second pulses overlapped, by removing the activity associated with the first pulse from the P2-evoked traces, including baseline trends (see Fig. S4). The qualitative patterns did not vary if this correction was not applied (*see* Fig S5). Note also the difference in the y axis scale compared to panels A,C. **F,H.** Standardized regression coefficients (mean ±SEM) illustrating the effect of P1 (*solid line*) and P2 (*dashed line*) coherence on evoked CPP-P2 amplitudes. Inset topographies illustrate the difference between [P1 high – P1 low], solid outline; [P2 high – P2 low], dashed outline) [0.4-0.6s] after P2. The negative effect of P1 illustrates higher amplitudes for P1-low trials. *Markers along the bottom of panels B,D,F and H indicate significant clusters where coherence effects differed from zero (two-tailed cluster-based permutation test, p<0.05). Shaded areas indicate the tested time window. See Fig. S3 for full-trial ERP traces, sorted by gap and coherence conditions.

further modelling approaches to attempt to capture them in the current study (but see Fig. S9, *S10* and *S11* for exploratory analyses on how temporal expectations might influence integration processes and evidence weighting).

Then, we simulated, from this diffusion model fit to accuracy data, the neural activity corresponding to MBL and the CPP (Fig. 5). Our empirical results suggested that motor preparation as indexed by MBL tracks the state of the bounded decision variable in a sustained manner, emerging shortly after the first pulse and remaining lateralised until response. Thus, we simulated MBL by taking the signed values of the model-derived DV throughout the trial and averaging across trials. These exhibited a similar pattern to the empirical data, with the signed DV showing opposite-sign patterns for error vs. correct trials (Fig. 5A,D, *top; cf.* Fig. 2A). If a bound was hit, the DV was set to stay stable in our model, and therefore recapitulated the way in which motor preparation responses here (Fig 2A) and in previous studies (e.g. (Donner et al., 2009; Murphy et al., 2021; Parés-Pujolràs et al., 2025; Twomey et al., 2016) sustain until response execution. Note that, in our simulations (Fig. 5A,D), the average traces do not always reach the estimated bound: this is because, in a fraction of trials, the bound was never hit, bringing averaged values away from the bound value.

In turn, our results suggested that the transient CPP activity reflected local, pulse-driven accumulation fed to the DV while evidence was present. This accumulation process stopped during incoherent random dot intervals, leading to the signal falling down rather than maintaining the global DV state. Thus, we simulated CPP activity by taking the absolute values of the cumulative evidence gathered within each pulse ($|\Delta DV|$) on single trials (in keeping with the always-positive nature of the CPP; see Afacan-Seref et al., 2018; Kelly et al., 2021) and averaging across trials. If a bound was hit by the overall DV, the CPP traces were set to return linearly to 0 within 200 ms, as empirically observed in action-locked traces in self-paced tasks (e.g. Steinemann et al., 2018), and it did not resume upon presentation of a second pulse. This fall-down is only a signal feature accompanying the deactivation of the intermediary integration process and does not bear on choice. Given that the CPP traces in our grand-averaged data (Fig. 2B) fell fully back to baseline by the end of the longer gaps, CPP traces were also assumed to linearly return to zero as soon as the dots turned blue at the end of evidence pulses if a bound had not been hit by that time. Such a pattern assumes that the CPP generators are active during periods where evidence is presented (yellow dot pulses), but become inactive and fall down to baseline once evidence stops (blue dot periods). During pulse processing, the CPP feeds its output to the downstream motor level, which sustains its current level during the gap rather than deactivating. In this way, the motor process continuously represents the overall DV throughout the trial: the evidence that had been integrated by the CPP during pulse 1 (ΔDV_P1) is maintained at the motor level through the gap, is potentially updated by another round of accumulation by the CPP during pulse 2 provided the bound was not already reached, and thereafter further sustains up until response execution. Given the absence of previous empirical data on how signals may fall down without having hit a bound, we assumed the same fall-down rate in this case as when a bound is hit (linear return to zero within 200 ms).

The simulated single-pulse accumulation traces from our model captured the sensitivity of both CPP-P1 and CPP-P2 to motion coherence. The difference in CPP-P1 slopes for high vs. low coherence pulses is simply explained by the high vs. low drift-rate associated with these conditions (Fig. 5B,E). In the more complex case of CPP-P2, the activity evoked by P2 reached higher amplitudes in trials where P1 was low coherence (Fig. 5C,F). Our model can account for this due to two effects: First, because P1-Low trials are less likely to terminate early (Fig. 4B), and therefore fewer trials take a value of zero during P2. Second, because among those trials that do not terminate early, the level reached by the DV by the end of pulse one (ΔDV_P1) is on average lower for low- than high-coherence (Fig 4C; Fig 5B,E), and therefore more evidence from P2 needs to be integrated before the bound is hit and accumulation terminated. Thus, the higher CPP-P2 amplitudes reached in trials with low P1 coherence reflected both a higher proportion of trials where participants engaged in accumulation of P2, and the fact that they had to cover a longer distance to reach the bound (i.e. larger changes in the DV ($|\Delta DV\_P2|$) were possible before a bound was hit).

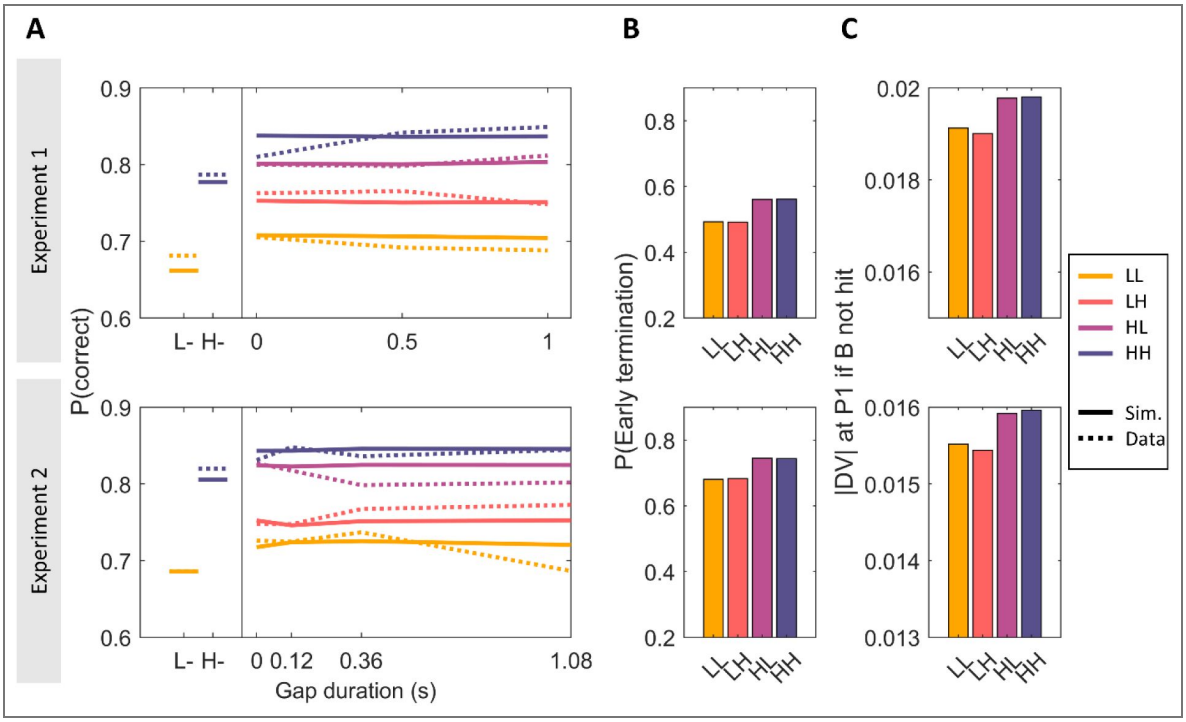

Figure 4. Simulated behavioural data

(N = 50000) of a simple bounded accumulator model with three parameters (B (bound), d1 (low drift rate), d2 (high drift rate)), fit to all grand-averaged data points for each experiment separately (see Fig. S12 & Fig. S13 for results based on single-participant fits). **A.** Grand-averaged simulated (*solid lines*) accuracy in single- (*left*) and two-pulse (*right*) trials, sorted by pulse coherence and gap duration in experiments 1 (*top*) and 2 (*bottom*). Observed data are overlaid (*dashed*) for comparison. Simulated data recapitulated the observed order effects. For simplicity, the model was not endowed with any means to account for effects of gap duration. **B.** Proportion of simulated two-pulse trials that hit a bound during the first pulse, and therefore did not use the second pulse evidence to make a choice. **C.** Absolute value of the decision variable (DV) at the end of pulse 1 in the subset of trials where the bound was not hit during that pulse, sorted by condition.

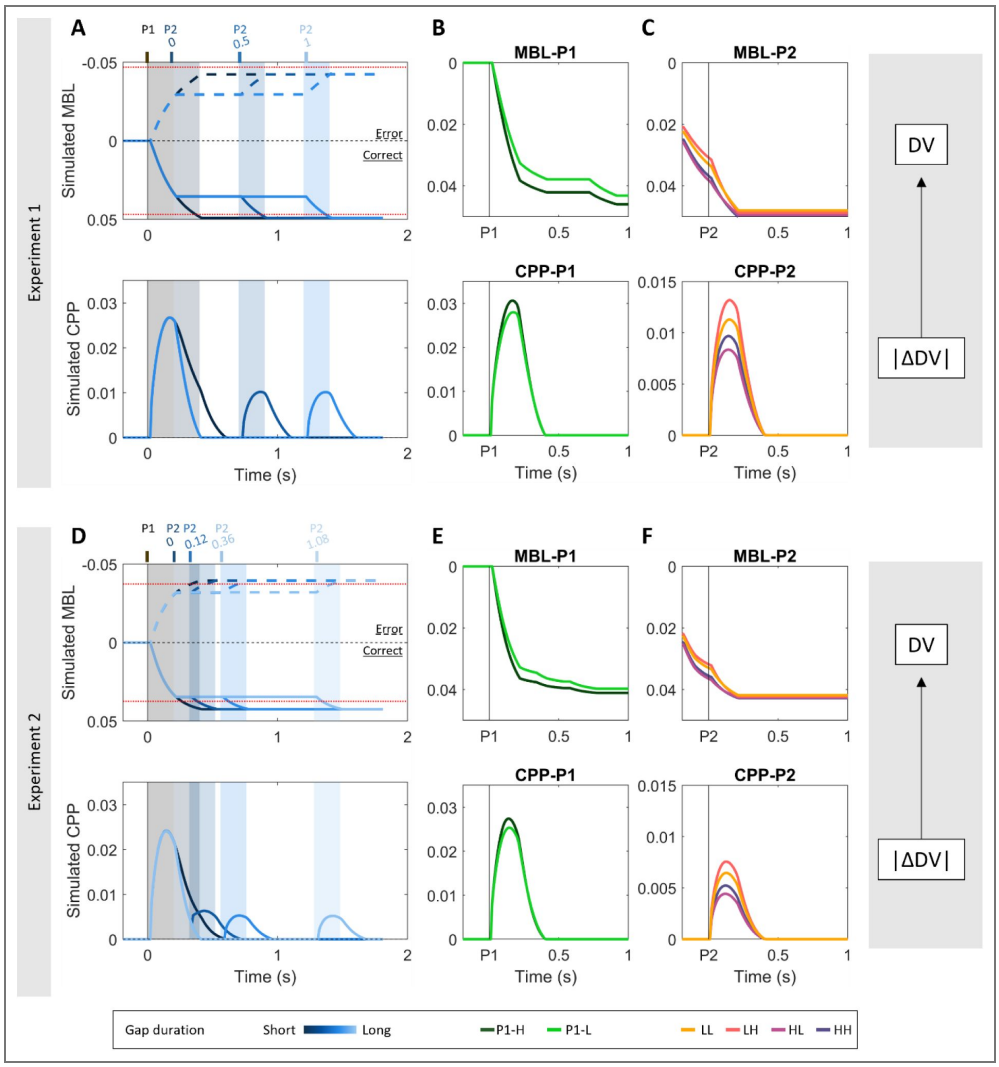

Figure 5. Model-derived simulations of motor beta lateralisation (MBL), reflecting the overall 'DV', and centroparietal positivity (CPP), reflecting local pulse accumulation (|ΔDV|) recapitulate empirical data.

A,D. Simulated average MBL (*top*) and CPP (*bottom*) traces over the whole trial, sorted by gap duration. MBL traces are additionally sorted by accuracy (solid line = correct; dashed lines = error). The simulations recapitulate the bimodal shape of the CPP across the whole trial, with the second pulse reaching lower amplitudes than the 1st one in both experiments (see Fig. 2B). In turn, by assuming that MBL signals track the state of the DV throughout the trial and because no leak or decay is assumed, our simulations could also recapitulate the sustained nature of motor lateralisation signals throughout the gap. Note that DVs were simulated so that positive signs are associated with correct choices, and negative signs to errors (hence the y-axis inversion to accord with empirical MBL signals). Dotted red lines indicate the bounds for error/correct trials, respectively. **B,E.** Simulated MBL-P1 (top) and CPP-P1 (bottom), sorted by P1 coherence, and averaged across all gap durations and accuracies. Note that the step-like changes in MBL traces are due to averaging the DV values over the various gap durations. No such effect is observed in simulated CPP potentials because traces are derived from P1 activity exclusively. **C,F.** Simulated MBL-P2 (top) and CPP-P2 (bottom), sorted by P1 and P2 coherence, and averaged across all gap durations and accuracies. Our simulations recapitulate the observed coherence effects at both CPP-P1 (see Fig. 3A,C) and CPP-P2 (see Fig. 3E,G). Note that, for CPP simulations, we plot the estimated build-up at P2 assuming that activity started at 0 and not considering any potential overlap from post-P1 fall-down earlier on in the simulated trial, for consistency with the empirical traces where CPP-P1 activity is removed from the P2-evoked traces. In contrast, the MBL-P2 traces continue from their post-P1 state, accounting for the sustained nature of the signal (see Fig. S2,*S3* for empirical MBL-P1/P2 traces). Note also that, for the sake of simplicity, our CPP simulations do not assume any delay between stimulus presentation and signal build up. Therefore, our simulated CPPs start building up immediately after pulse onset, while empirical ones start with approximately a 0.2s delay. Similarly, although motor preparation signals lag the motor independent buildup dynamics at the CPP level, we assumed instant transmission here for simplicity. Since only accuracy and not reaction time was to be captured in the modelling of this delayed-response task, it was not necessary to estimate transmission delays.

The model also predicted differences in CPP amplitude in correct/incorrect trials, which our dataset broadly recapitulated (Fig. S6). In particular, it predicted stronger CPP-P1 coherence-dependent effects in correct vs. incorrect trials, and it also predicted an interaction between accuracy and P2-coherence on CPP-P2 amplitude in trials with mixed coherences (HL, LH).

Finally, we assessed the extent to which some of our models' assumptions influenced the simulated CPP profile. For example, we assumed for parsimony that the CPP would deactivate with the same temporal dynamics when a decision process terminates because a bound has been hit, as when accumulation is reset at the start of the gap, but we do not know this to be the case. In fact, our simulations show the CPP falling down rapidly to baseline in all gap conditions, while empirical data show the CPP reaching all the way to baseline for the longest gap condition only. We therefore conducted additional simulations to illustrate how different assumptions about the fall-down duration (i.e. time to go back to 0) and delay-to-fall (i.e. the amount of time elapsed before the signal stops accumulating and starts going down) would affect the CPP's profile during the gap in our two experiments (Fig. S7). These parameters affected the CPP shape during the gap, but the patterns of coherence-dependent CPP-P1 and CPP-P2 amplitudes remained unchanged. Longer fall-down durations better recapitulate the observed empirical fall-down in short gap conditions, where signals fail to reach baseline before the second pulse onset. These simulations suggest that our assumption of a 200ms fall-down time may have underestimated that of the true signal dynamics, but dedicated experiments will be required to precisely quantify the fall-down characteristics of the CPP in these scenarios. In turn, allowing for some post-decisional evidence accumulation before the signal starts falling down also better captures some features of our empirical data, such as the higher amplitudes and longer peak latencies observed in the zero gap condition (Fig S7). We also simulated an alternative scenario where the signal is not assumed to fall (Fig. S8), which would be predicted if the CPP's neural generators remained active throughout the gap, encoding a sustained representation of the DV, so long as the bound has not been crossed. These simulations did not recapitulate the CPP's full drop to baseline in the long gap conditions, and produced distinctly smaller CPP-P2 evoked potentials relative to CPP-P1 (Exp. 1: CPP-P2 = 19% of CPP-P1 amplitude; Exp. 2: CPP-P2 = 13% of CPP-P1 amplitude) than observed in the empirical data (see Fig. 2B), which were more closely approximated by the model assuming a full reset during the gap (Exp. 1: CPP-P2 = 53% of CPP-P1 amplitude; Exp. 2: CPP-P2 = 35% of CPP-P1 amplitude; see *Methods* for full details on this analysis). Thus, the data are more consistent with a full reset of the intermediate accumulation process reflected in the CPP at the end of the pulse containing informative evidence, regardless of it having crossed a bound, with the maintenance of intermediate, potentially subthreshold levels of the overall DV being encoded solely at the downstream level of motor preparation.

3. Discussion

A wealth of studies has investigated the neural mechanisms underpinning evidence accumulation in tasks where information is continuously available, identifying multiple neural decision signals at various levels in the sensorimotor hierarchy (Gold & Shadlen, 2007; Heekeren et al., 2008; O'Connell & Kelly, 2021; Okazawa & Kiani, 2023). However, little is known about the mechanisms underpinning decision-making in contexts where evidence from a given source comes in temporally separate bouts. This is important not only because many real-life decisions require this kind of integration, but also because neural decision signals can exhibit functional dissociations when probed in more complex contexts (Okazawa & Kiani, 2023; Parés-Pujolràs et al., 2025). In this study, we asked: how do neural decision signals support evidence accumulation if information availability is paused for a variable amount of time? Focussing on two human EEG decision signals, the centroparietal positivity (CPP) and motor beta lateralisation (MBL), we show that they reflect processes with distinct roles during decision formation in this context. Across two experiments, we show that the CPP does not exhibit sustained activity during the gap between evidence pulses, but exhibits transient build, peak and fall dynamics in response to each pulse that track distinct rounds of evidence accumulation, and reflect the absolute contribution of each pulse to the overall decision variable ($|\Delta DV|$). In contrast, MBL exhibited build-up during pulses and sustained activity during the gap between, consistent with the

encoding of a signed DV evolving across pulses. Our behavioural and neural data can be explained by a simple bounded accumulation process, where participants sometimes terminate decisions early despite a cost in accuracy.

Our finding that the CPP exhibits transient activations tracking multiple rounds of evidence accumulation that feed into a single decision provides further insight into its functional role. Most previous studies using continuous evidence paradigms showed that the CPP steadily grows throughout an evidence accumulation process, in parallel with motor preparation, consistent with its reflecting the absolute value of an underlying, continuously-accumulating DV (Kelly & O'Connell, 2013; O'Connell et al., 2012; Steinemann et al., 2018). In contrast, in our task the CPP exhibits two distinct build-up processes that align with the two pulses presented in each trial. This suggests that the CPP builds up while accumulation is ongoing, and disengages when the accumulation process is paused or a bound is hit. This interpretation of our data was further supported by simulations of the CPP profile under various signal decay assumptions, which showed that empirical signals were better recapitulated by a process that assumes that the CPP signal falls down toward baseline when evidence is paused (Fig S8). Furthermore, we observed that the amplitude of each pulse-evoked CPP reflected the weight of that pulse on choice. At the grand average level, the initial pulse systematically evoked higher amplitudes than the second one, consistent with its greater influence on choice behaviour (Fig. 2B). Further, single-trial regressions confirmed that fluctuations in CPP-P1 amplitude for a given coherence level were linked to behavioural variability, with higher-than-average CPPs associated with a stronger weighting of the first pulse on choice (Fig S11). Put together, these results are suggestive of a direct link between the CPP amplitude following a particular stimulus and that stimulus' weight on choice. Empirical observations from previous studies align with this interpretation. In a previous study using the same gaps task (Azizi & Ebrahimpour, 2023), it was the second pulse that had a stronger weight on choice rather than the first (discussed below), and we note that CPP amplitudes were accordingly larger for pulse 2. Thus, although the direction of the behavioural bias differed across studies, in both, the bias in CPP amplitudes was in the same direction as the behavioural bias.

Our results support the idea that the CPPs following sequential pulses capture multiple rounds of evidence accumulation that are part of a single decision, and that its amplitude reflects each pulse's partial contribution to an evolving DV. In contrast to the transient pattern of activity that characterises the CPP in our task, MBL started shortly after the first pulse, and was sustained at a coherence dependent level throughout the whole trial duration (Fig 2 & Fig S2). This is in line with multiple previous studies, which have identified sustained encoding of decision variables in motor preparatory signals (Donner et al., 2009; Murphy et al., 2016, 2021; Parés-Pujolràs et al., 2025; Wyart et al., 2015). Put together, our findings support the idea that in this task the CPP feeds to accruing evidence from each individual glimpse of evidence ($|\Delta DV|$) to downstream motor signals that maintain a sustained representation of the evolving DV. Thus, our study identifies new task-dependent functional dissociations between distinct levels of the neural architecture underpinning decision making.

The dynamics within these levels and interactions between them were further illuminated by our computational models. In our two experiments, both the behavioural and neural effects could be reproduced with a two-level bounded accumulation model, in which an intermediate accumulator operates locally on contiguous periods of evidence, feeding its output on to a thresholded motor level where the cumulative total is sustained. Our model assumed that participants stop accumulating evidence if a bound is hit and that accumulation is paused during the gap between pulses; while the cumulative total is held at the motor level, the intermediate accumulator resets. By assuming that the CPP becomes inactive and falls down during the gaps, our simulations could recapitulate key CPP characteristics observed in our task including the opposite effects of the first and second pulse coherence on its amplitude. The fact that trials with low coherence first pulses were less likely to be terminated early, and had to cover a longer distance-to-bound upon presentation of the second pulse explained why CPP-P2 reached higher amplitudes in those trials.

A key feature of our model which enabled it to account for our behavioural observations was that accumulation was bounded, so that decisions could be terminated before all of the evidence has been sampled and accumulated. Given that the motion in any two sequential pulses in the gaps task always went in the same direction, that behavioural responses were deferred until a later cue, and that single-pulse accuracies were far from ceiling, the optimal strategy would have been to perfectly accumulate all available evidence; by setting a bound, our participants often missed some information and thus achieved suboptimal accuracy. While behaviour approximating perfect integration in relatively long timescales has been reported across species (Brunton et al., 2013; Waskom & Kiani, 2018), suboptimal integration is frequent. Previous expanded judgement tasks prescribing perfect integration have often reported recency biases (Cheadle et al., 2014; Wyart et al., 2015), but primacy effects consistent with early decision terminations have also been observed in both humans (Balsdon et al., 2020) and non-human primates (Kiani et al., 2008; Mazurek et al., 2003; Yates et al., 2017). Some studies have even found "bump-shaped" psychophysical kernels indicating increased weighting of evidence occurring around the middle of a stimulus sequence (Keung et al., 2019, 2020; Sospedra et al., 2025). Such deviations from optimal integration may reduce cognitive effort at the cost of accuracy, and may emerge due to multiple factors, including stimulus properties (Bronfman et al., 2016; Lange et al., 2021), biases driven by stimulus consistency (Cheadle et al., 2014; Glickman et al., 2022) or choice history (Urai et al., 2019), or result from different integration strategies that may be flexibly deployed, such as leaky (Tsetsos et al., 2012) or bounded accumulation (Kiani et al., 2008; Mazurek et al., 2003).

In the context of our task, previous studies using the same stimuli found the opposite bias in behavioural weighting, where the second pulse had a stronger influence on choice than the first (Azizi & Ebrahimpour, 2023; Kiani et al., 2013). Given that the stimulus characteristics (dot speed, density) in previous work were the same as in our study, differences in trial structure, difficulties and training may account for this discrepancy instead. For example, our task had comparatively long lead-in periods before the first pulse (min. 0.7s compared to min. 0.4s of previous studies), which may have helped them to prepare for full integration of the first pulse. We also used a narrower range of coherences than the previous studies, which possibly lends itself to calibrating a bound to achieve acceptable accuracy while saving cognitive effort. Furthermore, we did not use trial-by-trial feedback but rather provided aggregate performance metrics at the end of each block, which would have detracted from participants' ability to monitor their own performance. Finally, even though the probability of a single pulse trial was the same, the single-pulse staircasing procedure we used at the beginning of the task may have encouraged a strategy more focused on the information in the first pulse. In line with this interpretation, a recent study that also lacked trial by trial feedback and used a single-pulse training procedure has also reported recency effects in a task with different visual stimuli but the same variable-delay task structure (Golmohamadian et al., 2025). However, resolving the factors that encourage early termination strategies will ultimately require dedicated experimental manipulations.

Our findings regarding the CPP's contribution to decisions based on temporally separate bouts of evidence aligns with the results of recent work in expanded judgement tasks (Parés-Pujolràs et al., 2025; Wyart et al., 2012, 2015). In expanded judgement studies, participants view a sequence of discrete, easily-identified tokens that support one of two choices and must integrate over multiple tokens to make an accurate decision. In these tasks, CPP responses to discrete tokens have been shown to scale with context-optimal belief updates in classic non-volatile contexts that prescribe perfect linear accumulation (Wyart et al., 2012, 2015) as well as in volatile environments where the correct answer may change within a given trial, which prescribe a nonlinear transformation of the token information being integrated (Parés-Pujolràs et al., 2025). That is, evoked CPP activities track how much a DV changed following each piece of evidence, but not the absolute running sum of accumulated evidence. This stands in contrast to the results from conventional decision-making tasks where evidence is presented continuously, and in the form of high-noise continuous stimuli (Geuzebroek et al., 2023; Gherman et al., 2024; O'Connell et al., 2012; Steinemann et al., 2018) rather than low-noise discrete tokens. Our task represents a middle ground between these two types of paradigms: we used noisy continuous evidence, but

grouped it in two temporally discrete, sequential windows. Thus, participants needed to integrate over time to discriminate the information in each evidence pulse, but also across evidence pulses to maximise their accuracy. This allowed us to show that, in conditions where evidence is noisy and continuous but can be paused, the CPP's profile separately tracks multiple rounds of evidence accumulation. When such updates occur in discrete steps as in expanded judgement tasks, or in short dynamically-accruing bouts as in our gaps task, the CPP does not seem to keep track of the state of an overall DV between temporally separated pieces of evidence, but rather processes each piece separately. However, it remains unclear to what extent the CPP may behave differently in other contexts. In particular, a common feature between expanded judgement tasks and our design is that the presence of evidence is unambiguously indicated, in our case by colour cues. These colour cues may have acted to trigger initiation and termination of two rounds of evidence accumulation. However, it is plausible that in the absence of such external cues the CPP may have exhibited a sustained pattern of activity consistent with continuous monitoring of the environment (Geuzebroek et al., 2023), potentially plateauing during periods with incoherent dot motion that should elicit close-to-zero, or heavily reduced, momentary belief updates on average. This will require a dedicated experiment to test.

Our study also leaves some open questions. Given that the coherence-dependent effects of gap duration on behaviour were not expected and were inconsistent across the two experiments (Fig 1B), we did not aim to capture them in our modelling. However, surmising that they might relate to dynamic expectations arising from the temporal structure of the task, we sought to gain insight into dynamics of attentional engagement and expectation through exploratory analyses of occipital alpha activity (Fig 2C, Fig S9). Occipital Alpha-band power has been linked to attention and temporal expectations (Rohenkohl & Nobre, 2011), and also to the onset (Van Den Brink et al., 2021) and build-up rate (Kelly & O'Connell, 2013) of evidence accumulation signals like the CPP. In our two experiments, the gap durations between the two pulses followed different distributions: in Exp 1 gaps were uniformly distributed, whereas in Exp 2 they were skewed towards shorter gaps durations. We found evidence that occipital alpha power was sensitive to this difference (Fig S9), in that it was relatively reduced during the longer gaps in Exp 1, where they were relatively more likely, compared to Exp 2. We also found that phasic alpha decreases additionally modulated the weight of the second pulse on behaviour in Exp 2 (Fig S11), suggesting that phasic alpha activations may influence evidence integration. However, more work is required to specifically test how tonic and phasic occipital Alpha may interact with evidence accumulation processes, or influence behaviour through other mechanisms.

In sum, our study provides novel insight into the neurocomputational mechanisms supporting decision making in a context where decisions need to be made on the basis of a single stimulus feature that is only intermittently available. Our task allowed us to identify novel functional characteristics of a well-established neural decision signal in the human EEG: the CPP. We show that in tasks where perceptually noisy evidence is presented intermittently in short bouts, the CPP does not maintain a sustained representation of cumulative evidence, but rather engages in multiple rounds of evidence accumulation during those bouts, which in turn feed a continuously updating, sustained DV represented in downstream areas. This local evidence-processing property is consistent with recent work showing that the CPP encodes belief updates rather than the ongoing state of a DV in expanded judgment tasks involving the integration of a series of stimuli that are individually easy to identify (Parés-Pujolràs et al., 2025), and suggests that the CPP may only trace the entire evidence accumulation process underpinning decisions when the physical evidence is presented in one continuous stream (Geuzebroek et al., 2023; Kelly & O'Connell, 2013; O'Connell et al., 2012; Steinemann et al., 2018). Our results thus add to growing work suggesting that the neural architecture underlying evidence accumulation for decision-making can exhibit flexible functional roles in different contexts, underpinning adaptive behaviour.

4. Methods

Participants

Twenty-three participants were recruited to take part in Experiment 1, and 23 different participants were recruited to take part in Experiment 2 of this study. In Experiment 1, one participant withdrew after a few blocks of the task because they were feeling dizzy, and thus their data were excluded from further analysis. Two participants were unable to perform the task at the minimum required level of accuracy and were excluded from analysis in Experiment 2. A total of 22 (M = 21.5 years old, SD = 1.79 years old, 10 females) and 21 (M = 22 years old, SD = 3.85 years old, 11 females) participants were thus included in the final samples for Experiment 1 and 2 respectively. All participants provided informed written consent before participation in the study and were compensated for their time (10€/hour), and all procedures were approved by the University College Dublin Human Research Ethics Committee.

Task

Participants performed a motion direction discrimination task adapted from Kiani et al. 2013 using random dot kinematograms (RDK). The experiments consisted of a total of 700 (Exp 1) and 933 trials (Exp 2), divided into blocks of 70 trials each. Most trials in the experiment were two-pulse trials (85.7%) and the remaining fraction were single-pulse trials (14.3%). In single-pulse trials, the second pulse was not presented. Instead, the first pulse was followed by a 0% coherence lead-out period and then the trial terminated. The proportion of single- and two-pulse trials mirror the ones in the original Kiani et al. 2013 study.

Stimuli were presented centrally on a standard monitor, and participants sat at a 50-60cm distance from the monitor. Dots were presented within a 5° circular aperture at the center of the screen, the dot density was 16.7 dots/degree^2/s, and coherent dots moved at a speed of 5 degrees/s. Due to a technical error, the monitor refresh rate was 60Hz for 19 participants and 85Hz for 3 participants in Experiment 1, while it was 85Hz for 19 participants and 60Hz for 2 participants in Experiment 2. Each trial began with a white fixation cross presented at the centre of the display on black background. Then, a patch of 0% coherence dots appeared in blue colour on the centre of the screen (700 – 1050 ms, with short (700/750ms), medium (900/950ms) or long (1000/1050ms) delays appearing with a probability of 0.7,0.2 and 0.1, respectively). This was followed by a 200 ms pulse of yellow dots moving at either high or low coherence. After a gap of variable duration (Exp 1: [0, 0.5, 1] s, Exp 2: [0, 0.12, 0.36, 1.08] s) a second 200 ms pulse of either high or low coherence motion was presented. Finally, a patch of blue dots moving at 0% coherence was presented (700 to 1050 ms) in blue. The fixation cross was visible throughout the trial to encourage participants not to follow the dots with their eyes. At the end of the final blue dot sequence, all stimuli disappeared. Trials were separated by a fixed 1s intertrial interval. All gap durations were equally likely, and all possible motion coherence combinations (low-low, low-high, high-low, high-high) and gap durations were randomly permuted throughout the experiment. Three gap durations were originally used in Experiment 1 in order to maximise trial count for each of a small number of gap durations. Having observed that the participants utilised the second pulse less than the first, opposite to previous work (Kiani et al., 2013), we ran a second experiment with shorter gap durations made more prevalent, on the basis that closer temporal contiguity might make it less likely that participants would disengage from accumulation before the second pulse was presented and encourage continued accumulation. The expectations for a long gap to occur differed in our two experiments. Given the percentage of 1-pulse trials, if the second pulse had not yet occurred 500 ms after the 1st pulse the probability of it happening was higher in Experiment 1 (p = 0.666 [1/3*85.7/(1/3*85.7+14.3)]) than in Experiment 2 (p = 0.6 [1/4*85.7/(1/4*85.7+14.3)]. Participants were told they had to respond after stimulus offset, with no time limit. Participants responded by pressing the “C” or “M” keys on a standard keyboard with the left and right thumb respectively. The blue and yellow colours used in the experiment were selected to be physically isoluminant, as measured on the lab monitor, in order to avoid large evoked potentials arising from strong luminance changes.

Staircase procedure

In order to estimate the required dot coherence for participants to perform at 70% accuracy across coherence levels, all participants performed a staircase procedure consisting of 100 trials. All trials consisted of 0% coherence lead-in dots (700 to 1050 ms), a single pulse of evidence (200 ms) and a final sequence of 0% coherence lead-out dots (700 to 1050 ms). The staircase followed a 2-down, 1-up procedure (Levitt, 1971), and the starting value was set to 40% for all participants. After two correct responses, the coherence was lowered. The initial step size was set to 6%, and it was halved every second time the staircase went down. This was done to achieve greater precision towards the end of the staircase. The average coherence of the dot motion in the last 40 trials of the staircase procedure were used to estimate the two coherence strengths used in the task. Specifically, high (Exp. 1: M = 44.73%, SD = 12.64%; Exp 2: M = 33.04%, SD = 13.41%) and low (Exp. 1: M = 26.75%, SD = 7.74%; Exp 2: M =19.82%, SD = 8.04%) coherences were then set to be 25% higher or lower than the staircase-estimated coherence.

To keep performance constant throughout the task, the average accuracy was checked after each block and coherence was dynamically adjusted between blocks. If accuracy was on average lower than 60% or higher than 90% across conditions, coherence was adjusted by increasing or decreasing it by a tenth of the starting value obtained from the staircase procedure. This precaution was taken to avoid ceiling & floor effects. Most participants' performance was stable throughout the task, and only a few required substantial adjustments of coherence between blocks (see Fig. S1 for individual data).

EEG recording and preprocessing

Continuous EEG was recorded from 128 scalp electrodes using a BioSemi system with a sample rate of 512 Hz. Eye movements were recorded with four additional electro-oculogram (EOG) electrodes, two above and below the left eye and two at the outer canthi of each for vertical (VEOG) and horizontal HEOG) eye. Additionally, we recorded electromyogram (EMG) signals from the thenar eminence using two electrodes on the left and two on the right hand, as a standard procedure, though EMG was not of interest in the current study. All data were analysed in a Matlab R2021a using the EEGlab (Brunner et al., 2013; Delorme & Makeig, 2004) and the ERPlab plugin (Lopez-Calderon & Luck, 2014).

Continuous data were high-pass filtered at 0.1Hz, and low-pass filtered at 40Hz using a zero-phase shift Butterworth filter. Then, stimulus-locked epochs were generated from -1.5s to 3s around the onset of the first evidence pulse. Bad channels were defined as those exceeding 50 standard deviation units, and were interpolated. Data were then re-referenced to the common average of all EEG channels. Trials where participants blinked during one of the evidence pulses were excluded from analysis. Eye movements occurring at any other time during the trial were removed from the data using Independent Component Analysis (ICA). Epochs were baseline-corrected relative to the 200 ms before the onset of the first evidence pulse, and channels showing ±150μV deviations were interpolated on a trial-by-trial basis using the TBT toolbox (Ben-Shachar, 2018). If any given epoch had more than 20 bad channels, it was marked for rejection. Further, if any given channel was marked as "bad" on >30% of epochs, it was interpolated across the whole experiment. Finally, we applied a Current Source Density (CSD) transform (second spatial derivative) using the CSD toolbox (Kayser & Tenke, 2006) to the preprocessed data to reduce the spatial spread and thereby reduce overlap between topographic foci. Time frequency decomposition was performed using a 7-cycle morlet wavelet transform, extracted in 1-Hz steps in the 1-40Hz range. Alpha and beta band power were obtained by averaging power in the 8-12Hz and 13-30Hz frequency ranges, respectively.

Behavioural analysis

First, to investigate the effect of pulse coherence and gap duration on participants' accuracy, we ran the following logistic regressions on one-pulse (*Eq. 1*) and two-pulse trials (*Eq. 2*):

$$\text{Logit}(\text{ Accuracy }) \sim \beta_0 + \beta_1 p1\ \text{coh}\ + [\beta_{0,s} + \beta_{1,s} p1\ \text{coh}\ ] \tag{1}$$

$$\begin{gathered}\text{Logit}\ (\text{Accuracy})\ \sim \beta_0 + \beta_1 p1\text{coh} + \beta_2 p2\text{coh} \\ + \beta_3 Gap + \beta_4 p1\text{coh} * Gap + \\ + \beta_5 p2\text{coh} * Gap + \\ [\beta_{0,s} + \beta_{1,s} p1\text{coh} + \beta_{2,s} p2\text{coh} + \beta_{3,s} Gap + \beta_{4,s} p1\text{coh} \\ * Gap + \beta_{5,s} p2\text{coh} * Gap]\end{gathered} \tag{2}$$

Where terms between square brackets indicate random effects; *s* refers to each participant, and indicates that random effects (intercepts, or slopes) were calculated in addition to fixed effects for that particular coefficient. Next, to test whether participants were generally more accurate in two-pulse compared to one-pulse trials we ran the following logistic regression (*Eq. 3*):

$$\begin{gathered}\text{Logit}(\text{Accuracy})\ \sim \beta_0 + \beta_1\ \text{nPulses} \\ + \beta_2 p1\ \text{Coh}\ + \beta_3\ \text{nPulses}\ * p1\ \text{Coh} \\ [\beta_{0,s} + \beta_{1,s}\ \text{nPulses}\ + \beta_{2,s}\ \text{p 1 Coh}\ + \beta_{3,s}\ \text{nPulses}\ * p1\ \text{Coh}\ ]\end{gathered} \tag{3}$$

This analysis was restricted to two-pulse trials with equal coherences in the two pulses (HH, LL trials only) so that any effect of pulse number would be exclusively related to the presence of additional motion, rather than potentially capturing order or coherence-consistency related effects.

Then, to investigate the effect of pulse order on participants' accuracy, we ran the following regression (*Eq. 4*):

$$\begin{gathered}\text{Logit}(\text{ Accuracy }) \sim \beta_0 + \beta_1(p1\text{coh} + p2\,\text{coh}) + \beta_2(p2\text{coh} - p1\,\text{coh}) + \\ [\beta_{0,s} + \beta_{1,s}(p1\text{coh} + p2\,\text{coh}) + \beta_{2,s}(p2\text{coh} - p1\,\text{coh})]\end{gathered} \tag{4}$$

where the difference coefficient is expected to not be significant if the order of pulses does not influence performance.

In all regressions, coherence values were normalised within participant because they were staircased for each participant individually and varied widely. All models included a maximal random effects structure, with a random intercept and random slopes for all fixed effects to control for interindividual variability. All models were fit using the 'bobyqa' optimiser in the lme4 toolbox (Bates, 2011). In Experiment 2, this resulted in singular fits for both Eq. 2 and 3.

Following previous suggestions, we used a weakly informative prior to regularise the random effects covariance matrix (Chung et al., 2015) using the blme package (Chung et al., 2013), which resolved the singular fit problem. In cases where the model output flagged potential convergence problems, we assessed the robustness of parameter estimates by comparing them across 6 different optimisers using the 'allFit' function in lme4 toolbox (Bates, 2011), as advised by the developers. All such model fits were deemed to be robust as the optimiser estimates rarely deviated by more than one decimal point from the 'bobyqa' ones.

Finally, we compared participants' accuracy on two-pulse trials to the expected performance assuming perfect integration, and based on their accuracy in one-pulse trials. Following Kiani et al. 2013, we assumed that decisions are determined by the sign of the sum of evidence in the two pulses. The evidence distribution was inferred from participants' accuracy on single-pulse trials as follows:

$$\begin{gathered}e1 \sim \Phi^{-1}(P_1, 0, 1) \\ e2 \sim \Phi^{-1}(P_2, 0, 1)\end{gathered} \tag{5}$$

Where P1 and P2 are grand-average accuracies for high- and low-coherence one-pulse trials. **Φ** is the normal cumulative distribution function:

$$\Phi(x,\mu,\sigma) \sim \int_{-\infty}^{x} N(v,\mu,\sigma)dv \quad (6)$$

and $\mathbf{\Phi}^{-1}$ is its inverse. N(v,μ,σ) is the normal probability density function with mean (μ = 0) and standard deviation (σ = 1). The expected accuracy for double-pulse trials was then calculated as follows:

$$P_e \sim 1 - \Phi(0, e1 + e2, \sqrt{2}) \quad (7)$$

ERP analysis

CPP-P1 & CPP-P2 analysis

To investigate how centroparietal responses to the two sequential pulses varied with motion coherence, we extracted EEG activity from a cluster of centroparietal electrodes where activity at 500 ms after pulse 1 was maximal across conditions (see Fig 2). To compute CPP-P1 slopes, we fit a line from 0.2s post P1 onset when the CPP appeared to begin building, to peak time for each participant individually and for each P1 coherence condition separately, restricting the peak search times around [0.4-0.6s] post-P1. We then compared the slopes in those two conditions by running a paired-samples t-test. For CPP-P2 visualisation, we removed P1-related activity by subtracting the traces from the longest gap conditions [-0.2 to 1.4s with respect to P1], from all traces. This resulted in an average EEG activity of 0 (see Fig. S4) preceding the second pulse, in all conditions, and rendered the key CPP-P2 findings more clearly visible by removing P1-induced EEG drifts. Note that this does not affect the CPP-P2 activity in the long gap conditions, as the subtraction alters data up to the end of P2 but not further (see Fig. S4). We report the average across all non-zero gap conditions in the main manuscript (Fig. 2), as well as the data sorted by gap in the supplementary material (Fig. S3, *S4*). We also used the so-corrected activity to compare the relative amplitudes of CPP-P1 and CPP-P2 across all non-zero gap conditions. For this, we first computed the average amplitude 0.4 to 0.6s after P1 (in the raw data, $CPP\text{-}P1_{amp}$) and P2 (in the corrected data, $CPP\text{-}P2_{amp}$), for each gap separately, and averaged across all non-zero gap conditions. Then, we computed the percentage of CPP-P1 amplitude reached by CPP-P2 as $CPP\text{-}P2_{amp}/CPP\text{-}P1_{amp} * 100$.

To investigate the impact of dot motion coherence on both CPP-P1 and CPP-P2 amplitudes (Fig. 3), we ran a series of time-resolved regressions:

$$CPP_t \sim p1Coh + p2Coh \quad (8)$$

Where *t* indicates time from P1 for CPP-P1 analysis, and time after P2 for CPP-P2 analysis. For this analysis, we aligned all gap conditions to P1/P2 onset respectively and ran the regressions for all trials pooled, for each subject separately. For CPP-P2, data were additionally baselined using 100ms before P2 onset to minimise the impact of gap duration on average amplitudes. All EEG data were low-pass filtered (6Hz) prior to running the regression to reduce the impact of high frequency noise on these single-trial analyses.

Next, to investigate how trial-to-trial variability in attention and evidence accumulation influenced performance, we ran a series of time-resolved logistic regressions.

First, we investigated whether single-trial variability in centroparietal responses modulated the weight of pulses on choice. The interaction terms between pulse coherence and CPP amplitude in the following regression (*Eq. 9*) thus test whether pulses which evoked a particularly high centroparietal response were also associated with that pulse having a greater weight on choice:

$$\begin{aligned}\text{Logit}(P(\text{ Choice } = \text{ right })) \sim & \text{ p 1 Coh } + \text{ p 2 Coh } + \text{ p 1 Coh} \\ & * CPP_t + \text{ p 2 Coh } * CPP_t\end{aligned} \quad (9)$$

Where *t* indicates time after P1 for CPP-P1 analysis, and time after P2 for CPP-P2 analysis.

Second, we ran an analogous analysis to investigate whether fluctuations in evoked occipital alpha desynchronisation also modulated the weight of each pulse on choice (*Eq. 10*):

$$\begin{aligned}\text{Logit}(P(\text{ Choice } = \text{ right })) \sim & p1 \text{ Coh } + p2 \text{ Coh } + p1 \text{ Coh} \\ & * - \text{ Alpha } t_t + p2 * -Alpha_t\end{aligned} \quad (10)$$

Where *t* indicates time after P1 for alpha-P1 analysis, and time after P2 for alpha-P2 analysis.

All regressors and EEG signals were z-scored across trials by timepoint. For alpha power analysis, we took the *negative* alpha power across a range of bilateral occipital electrodes (see highlighted electrodes in Fig. 2), so that positive coefficient values indicate that higher attention (i.e. lower alpha power) increase weight on choice or CPP amplitude. For the CPP analysis, we used the signal averaged over a cluster of centroparietal electrodes for CPP (Fig. 2B). Regressions were run for each gap condition separately for times between [0-1s] after each pulse, and the resulting coefficients were aligned to P1 and P2 and averaged across conditions.

EEG statistics

EEG evoked potentials and regression results were statistically evaluated against zero using cluster-based permutations using the FieldTrip toolbox (Maris & Oostenveld, 2007; Oostenveld et al., 2011). All tests were two-tailed, cluster-corrected ($p<0.05$), and 10000 permutations were run. We additionally compared the magnitude of the occipital alpha level in the longest gap across the two experiments using an independent samples t-test in Matlab.

Model fitting & simulations

In order to account for participants' behaviour, we fit a simple diffusion model to the grand-averaged accuracy in the 4 conditions with three free parameters: bound (*b*) and two drift rates (*d1*, *d2*) corresponding to the low and high coherence conditions. The accumulator model followed this basic equation:

$$y_t \sim y_{t-1} + d + N_{0,\sigma} \quad (11)$$

Where yt is the accumulator output or decision variable (DV) for any time t within a pulse (where *d*=*d1* or *d* = *d2* depending on coherence). Gaussian noise, $N_{0,\sigma}$, was added in order to represent noisy sensory evidence through the trial. During the gap, the accumulator was set to stay stable at its final within-pulse value so that y_t was set to equal y_{t-1} for any time *t* outside of pulses during which incoherent motion was presented and dots were blue. Given the behavioural observation that overall accuracy did not decrease in longer gap durations, and the fact that evidence pulses were clearly indicated by a change in the dots colour, the DV was paused and not allowed to further accumulate the noise during the 0% coherence motion gap separating the two pulses. When the DV crossed a bound '*b*', evidence accumulation terminated. The accumulator assumed no noise or leak during the gap, and in any trials where the bound was not crossed accumulation continued upon presentation of the next pulse. Note that this one-dimensional, continuous, bounded accumulator represents the overall DV corresponding to the level of motor preparation. As we explain below, the CPP was simulated by extracting the single-pulse components of this model.

We fit the model by minimising G^2 with the *particleswarm* function in the Global Optimisation Toolbox for Matlab. G^2 is a goodness of fit measure that in this study quantified how much predicted accuracies differed from observed ones in each condition.

Computational models were fit to the two experiments separately simulating 10000 trials for each condition, and the best fitting parameters were then used to simulate CPP traces. Akaike Information Criterion (AIC) and Bayes Information Criterion (BIC) were computed to assess the goodness of fit as follows:

$$AIC = G^2 + 2 * k \tag{12}$$

$$BIC = G^2 + k * \log(n) \tag{13}$$

Where *k* indicates the number of free parameters for a given model, and *n* represents the number of trials used to fit the model.

Neural data simulation

We simulated MBL activity by taking the evolving value of the simulated decision variable throughout the trial. If a bound was hit, the DV was set to stay stable in order to account for the sustained nature of MBL signals our empirical data as well as previous work in delayed response tasks (Murphy et al., 2021; Parés-Pujolràs et al., 2025; Twomey et al., 2016).

In turn, following previous work, we simulated the CPP by taking the absolute value of the underlying, signed accumulator traces unfolding during each individual pulse, produced by the best fitting parameters of our model (Afacan-Seref et al., 2018; Kelly et al., 2021). Taking the absolute value implicitly assumes that the differential evidence accumulator is implemented via two separate neural populations that encode values respectively favouring one or the other alternative. If the simulated decision variable hit a bound, the accumulator traces were set to fall back down to zero within 200 ms after hitting the bound, based on past observations of post-peak CPP dynamics (Steinemann et al., 2018). In the model shown in the main text, if the overall DV did not hit a bound by the end of the first pulse, it was assumed that the cumulative evidence level attained thus far was sustained in the overall DV at the motor level, but that the intermediate accumulator fell back to its zero baseline level, and restarted accumulation upon the presentation of the second pulse, which at the motor level added to the already sustained level. Variants of this scheme were also explored, as explained in Fig. S7, *S8*. In order to qualitatively compare how well various decay parameters matched the empirical CPP dynamics, we computed the relative CPP-P2/CPP-P1 percentage amplitude predicted by various models by extracting the average evoked amplitude of the simulated CPP [0-0.2s] for each pulse separately, with respect to the pre-pulse baseline amplitude. This 0.2s interval is analogous to the time used for analysis of the empirical data (see above), but is set to an earlier time period because our simulations did not incorporate any sensory delay, and therefore ramping activity started instantly after stimulus onset.

Supplementary material

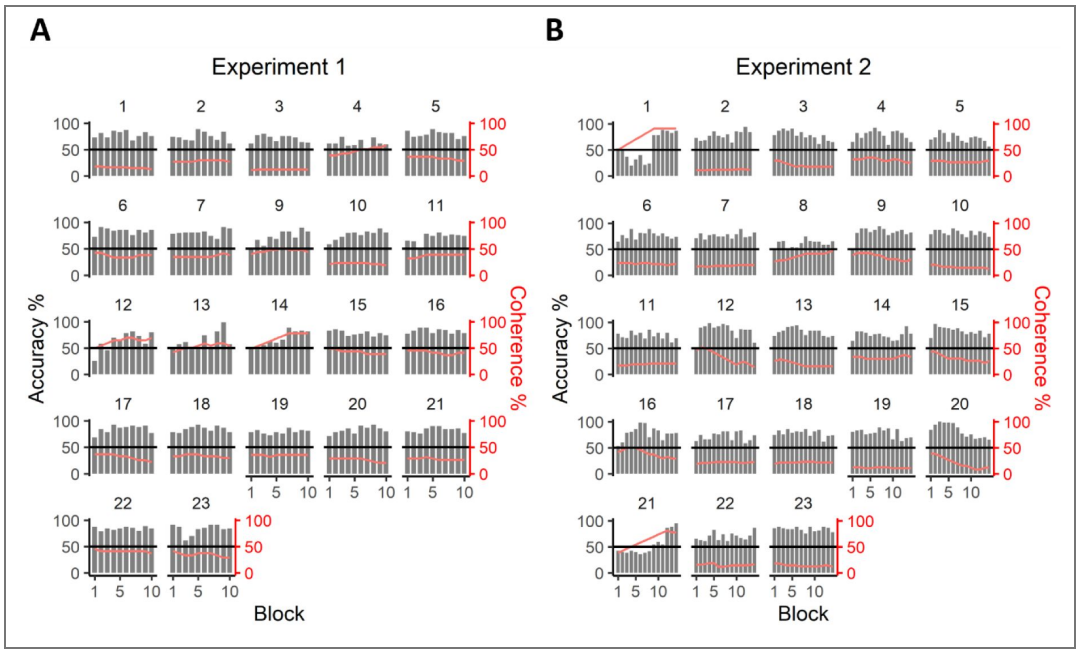

Figure S1. Individual participants' accuracy (*grey bars*) and average coherence (*red line*) for each block in Experiments 1 (A) and 2 (B). On average, most participants performed close to 70% accuracy and clearly above chance (*solid black line*), and only required minimal coherence adjustments between blocks. The data of participants 1 and 21 in Experiment 2 were excluded from further analysis due to poor task performance in a majority of blocks.

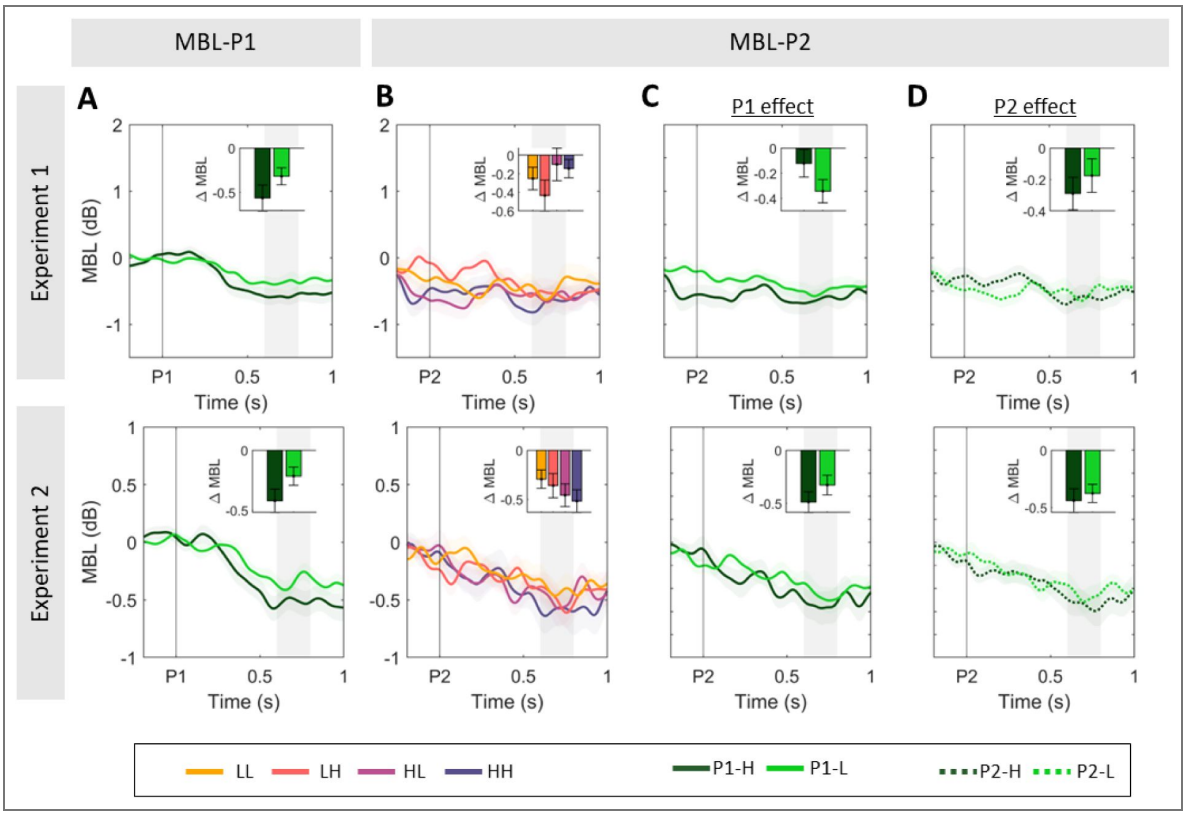

Figure S2. Sensitivity to evidence strength in the two pulses in motor beta lateralisation signals.

A. Grand-averaged (±SEM) motor beta lateralisation [Contra-Ipsilateral hemispheres with respect to correct response hand] after pulse 1 (MBL-P1), averaged across all gap conditions and across all trials regardless of accuracy. Motor preparation started shortly after the first pulse, and was sustained at a coherence-dependent level. **B.** Grand-averaged MBL after pulse 2 (MBL-P2), averaged over all non-zero gaps in the two experiments. **C.** Effect of P1 coherence on MBL after P2. Traces illustrate the grand-averaged (±SEM) aligned to pulse 2 (MBL-P2), averaged over all non-zero gaps and across P2 coherence. **D.** Effect of P2 coherence on MBL after P2. Traces illustrate the grand-averaged (±SEM) aligned to pulse 2 (MBL-P2), averaged over all non-zero gaps and across P1 coherence. In panels **A-D,** inset bar graphs illustrate the MBL excursion as the difference between activity at [0.6-0.8s, shaded area] after pulse onset, minus activity at baseline [-0.2-0s].

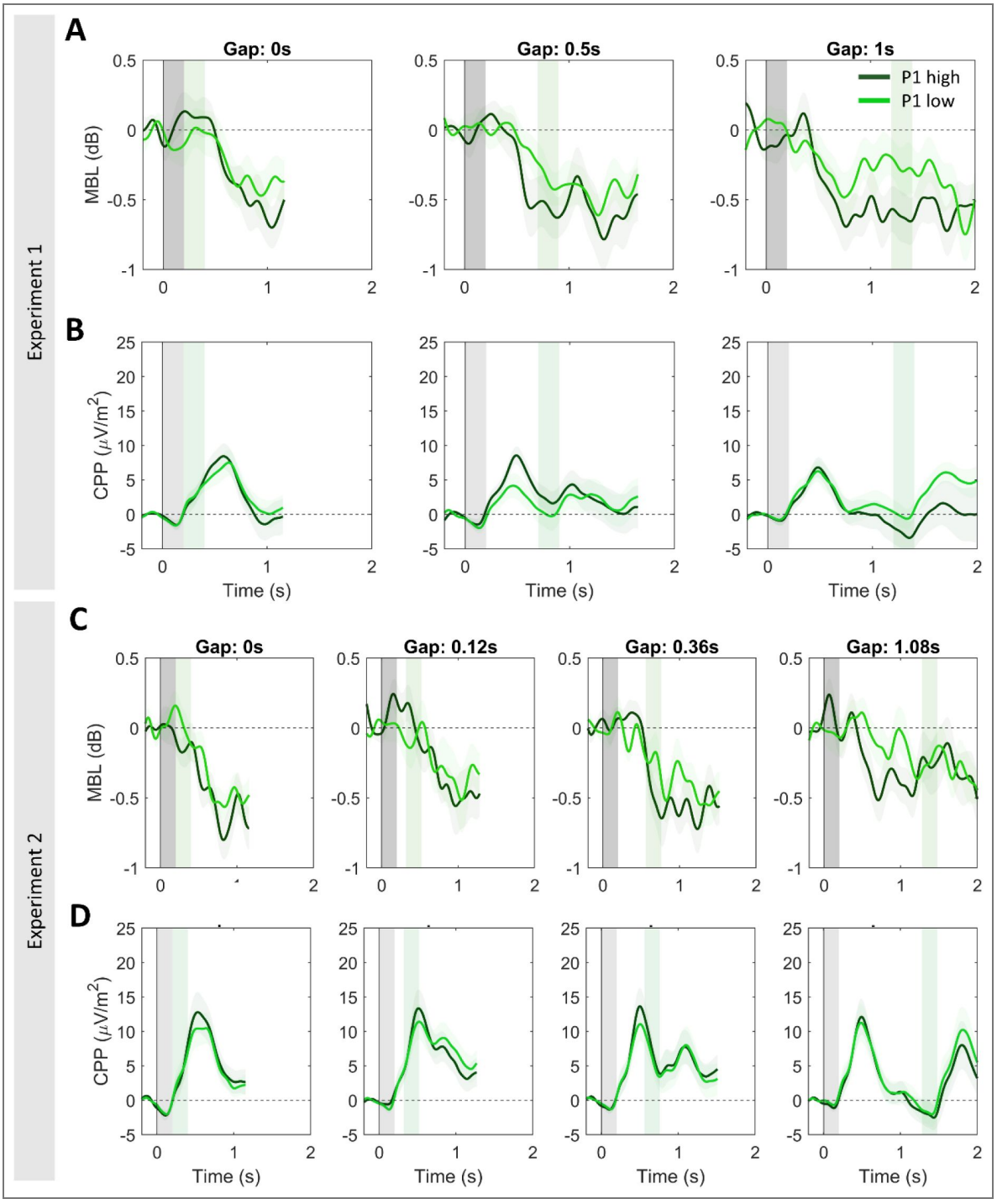

Figure S3.

A,C. Motor beta lateralisation (MBL) for each gap condition, sorted by P1 coherence in experiments 1 (A) and 2 (C). Lateralisation is computed as a function of actual dot motion [Contra-Ipsilateral hemispheres with respect to correct response hand], sorted by gap duration and P1 coherence pooled across correct & error trials. **B,D.** Centroparietal activity for each gap condition, and sorted P1 coherence in experiments 1 (***B***) and 2 (***D***).

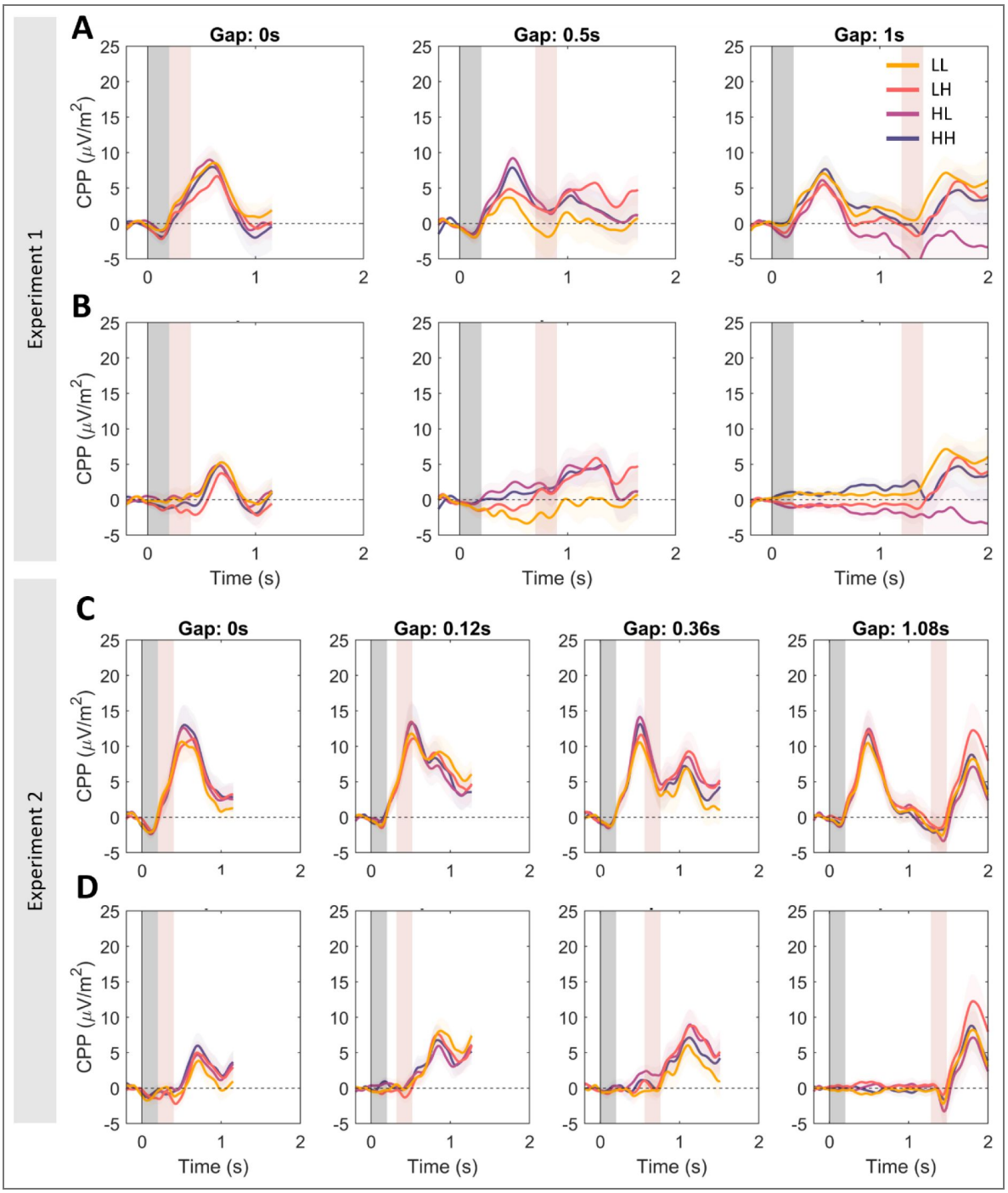

Figure S4.

A,C. Centroparietal activity sorted by gap, P1 and P2 coherence in Experiments 1 and 2. **B,D.** Centroparietal activity after removing CPP-P1 activity. For each condition, the average of long-gap trials with the same P1 coherence was removed. That is, the average of the long gap HH & HL conditions was subtracted from HH and HL traces. Similarly, the average activity of the long gap LL & LH conditions was subtracted from LL and LH traces. This removes overlapping CPP-P1 potentials, and isolates centroparietal activity related to P2. Subtractions were performed between [-0.2 to 1.4s] from P1 presentation. Thus, CPP-P2 potentials in the long gap condition remain unaltered.

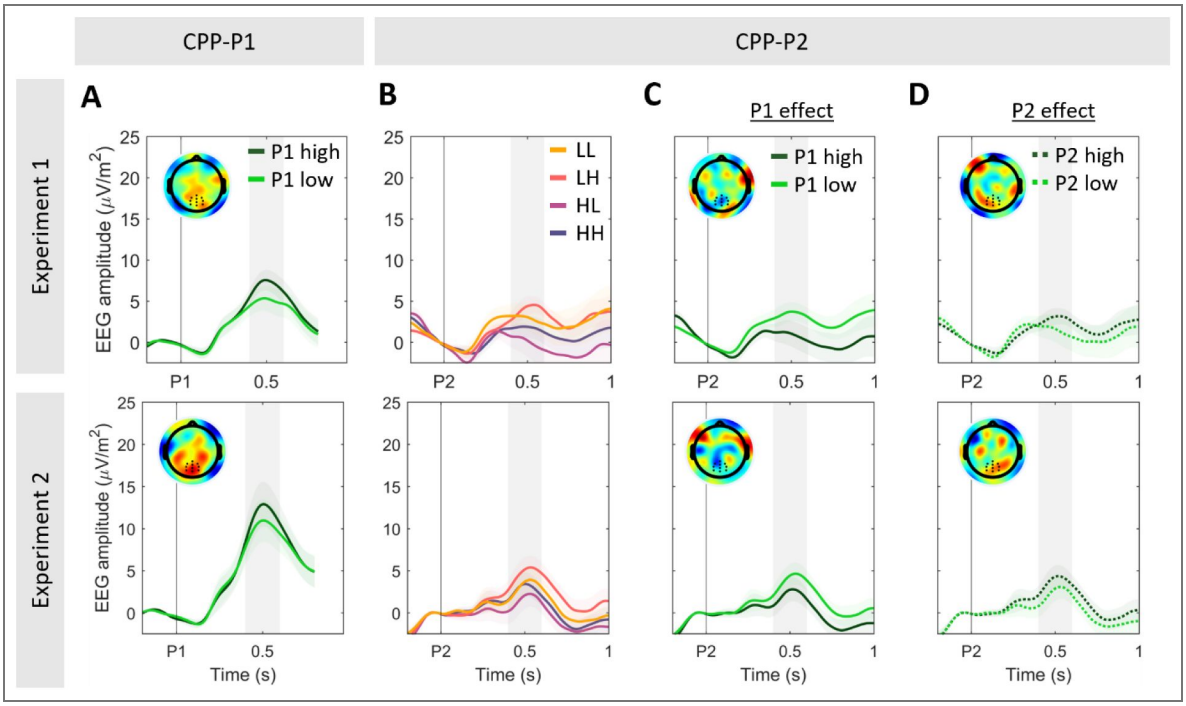

Figure S5. Replication of results in Fig. 3, now performing the analysis on CPP-P2 data (B-D) without removing CPP-P1 activity.

Note that baseline activity shows a drift consistent with the overlapping potentials from the preceding pulse, which is corrected for when removing CPP-P1 activity (cf. Fig. 3). Note also that the same patterns are qualitatively present in the uncorrected data. Panels C-D illustrate conditions pooled by P1 or P2 coherence, respectively, to highlight the different direction of the effect.

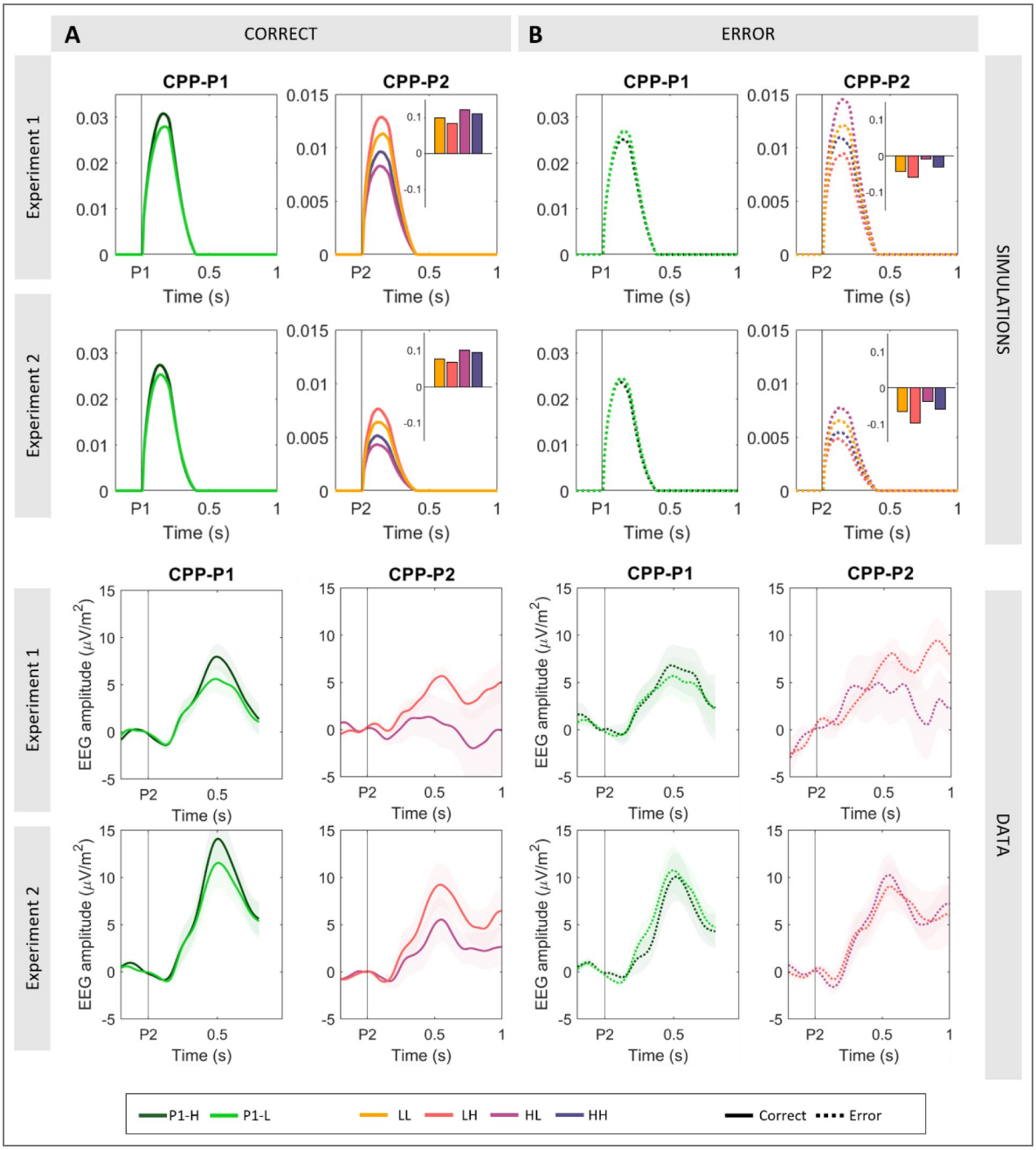

Figure S6. Model-predicted (A-B) and observed (C-D) CPP-P1 and -P2, in correct vs. incorrect responses, for Experiments 1 (top) and 2 (bottom).

Bar graph insets in A-B indicate the state of the simulated accumulator at the end of pulse 1 in those trials where the bound was not hit. Positive values indicate that the accumulator was leaning towards the correct answer, whereas negative values indicate that it was leaning towards an error. The model predicts stronger P1 coherence effects in correct compared to error trials (A-B, left), with this effect also being observed in empirical data across both experiments (C-D, left). For the sake of clarity, we do not plot LL and HH conditions in the empirical CPP-P2 data because no clear amplitude differences are predicted by the model in correct vs. error trials, and the trial count in the HH condition was insufficient in most participants. Further, the model predicted a strong interaction in CPP-P2 amplitudes in the HH vs. HL condition. While correct trials (which were the majority of trials in our task and the model) showed higher amplitudes at CPP-P2 for HL compared to the LH condition (A, right), consistent with the effect of P1 on CPP-P1 amplitudes reported in Fig 3, this effect reversed in incorrect trials (B, right). This interaction was also clearly visible in Experiment 2, although slightly less prominent in Experiment 1. Note however that Experiment 1 had fewer overall trials, and power to detect differences is likely to be insufficient after splitting conditions by accuracy.

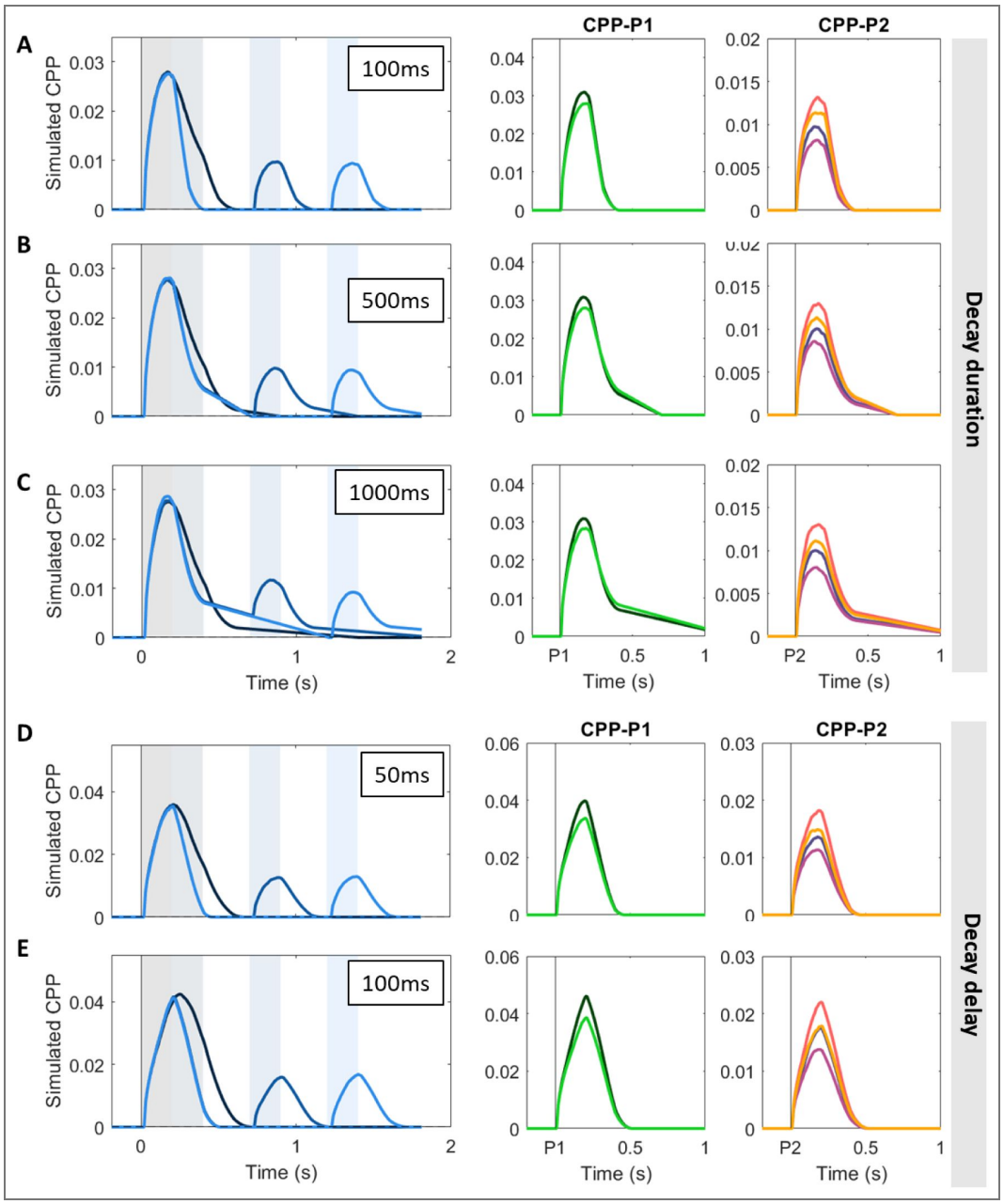

Figure S7. Simulations (N=1000) illustrating the effect of various signal decay time (A-C) and decay delay (D-E) assumptions on the predicted CPP activity.

Simulations are based on the fitted model in the main manuscript and for Exp. 1 only for illustration purposes. Given that it's unclear whether the CPP fall-down to zero when evidence is paused follows the same dynamics as its fall-down when it hits a bound (where studies with immediate behavioural responses suggest that it reaches zero within approximately 200ms; Steinemann et al 2018), we simulated its CPP activity under three different assumptions about the duration of its decay upon evidence interruption (i.e. when blue dots appear onscreen after a pulse). We simulated the CPP assuming the signal takes 100 ms (**A**), 500 ms (**B**) or 1000 ms (**C**) to go back to baseline at pulse offset when a bound had not been reached, retaining a 200 ms fall-down upon bound-crossing. Longer signal decay times for trials where no bound was hit result in a protracted ramp down to baseline. In turn, it is unclear whether any post-decisional evidence accumulation is to be allowed to simulate the CPP in this context, given that previous studies have observed varying delays in signal decay after response (Steinemann et al. 2018; Afacan-Seref et al., 2011). In the manuscript, we assumed no delay between bound crossing and signal decay. Here, we simulated the CPP allowing it to continue building up 50ms (D) or 100ms (E) after bound crossing, while setting it to immediately decay upon blue dot offset. Allowing some post-decisional build-up resulted in higher average CPP amplitudes, and it also better recapitulated some features of the data, including a protracted build-up in the zero-gap condition compared to all others.

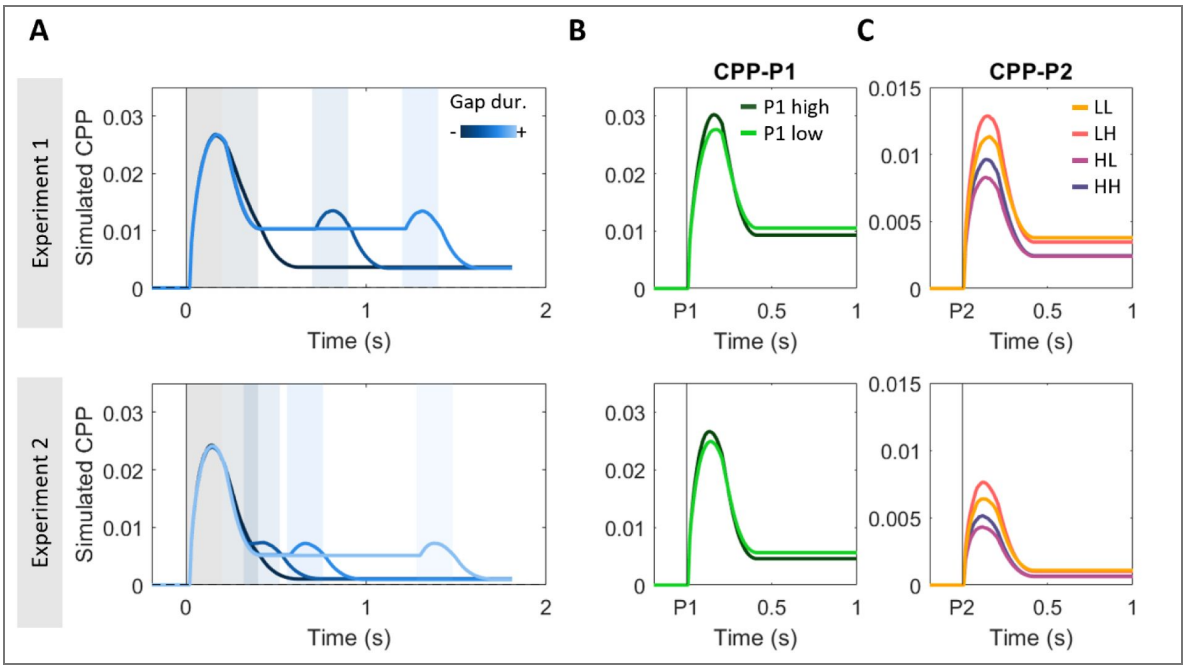

Figure S8. Simulated CPPs using the same computational model as in Fig. 5, but under the assumption that the signal was only reset to baseline if a bound was hit.

If the bound was not hit, the accumulator, like the downstream DV at the motor level, was set to stay stable at the final value reached by the end of pulse 1 with no decay and no added noise for the whole duration of the gap. Given that we do not model reaction times, we assumed no transmission delay between events on the screen and their impact on the accumulator. In this model, the partial fall down of the signal during the gap was driven by those trials that hit a bound following the first pulse. Conversely, the fact that it did not fall all the way to 0 on average during the gap is driven by those trials where the DV did not hit a bound during processing of pulse 1 and thus sustained through the gap. Accumulation resumed from that sustained level upon presentation of a second pulse, and the fact that on average CPP-P2 traces reach lower amplitudes than CPP-P1 evoked activities is explained by the fact that trials that were terminated during the first pulse did not engage in accumulation again, and therefore took value 0 in our model. Note that this model provides a qualitatively worse fit to the empirical CPP traces during the gap and CPP-P2 trials. In particular, the magnitude of the CPP-P2 potentials was predicted to be significantly smaller (Exp. 1: CPP-P2 = 19% of CPP-P1 peak amplitude; Exp. 2: CPP-P2 = 13% of CPP-P1 peak amplitude) than observed on the grand-averaged data (CPP-P2 = approximately 50% of CPP-P1 in both experiments; see Fig. 2).

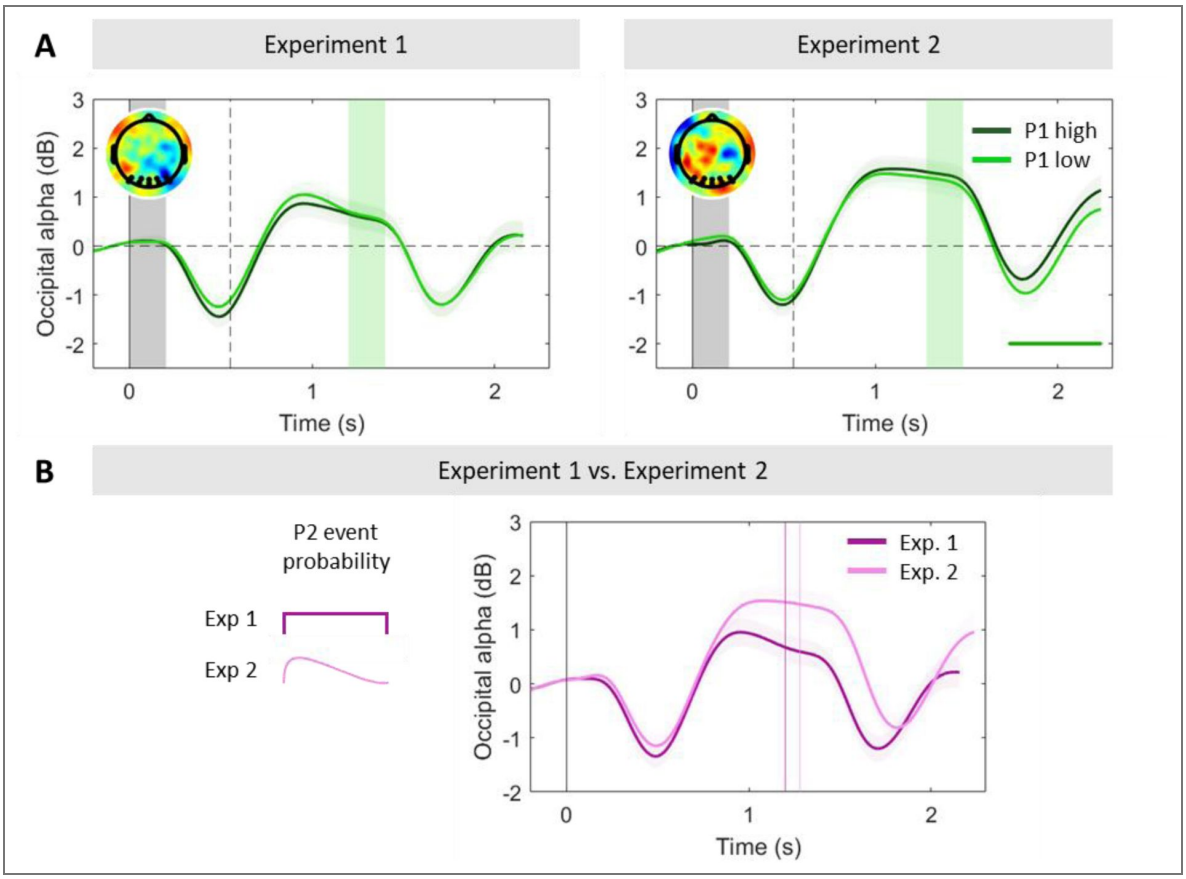

Figure S9. Occipital alpha power tracks dynamics of attentional engagement and varies with temporal expectations.

A. Grand-averaged (±SEM) occipital alpha power in the long gap conditions sorted by P1 coherence, again baseline-corrected before the onset of the first pulse. At evidence offset, alpha steeply increased, and, interestingly, attained and maintained a higher level during the longer gaps than the baseline before the first pulse (two-tailed cluster permutation test, $p < 0.05$ in both experiments; see Fig. 2A). One possible interpretation is that this reflects attentional disengagement from the decision occurring after early decision termination. However, if this was the case, we would expect this effect to be dependent on pulse 1 coherence, as it is more likely for a DV to have reached a bound after a high-coherence pulse (Fig. 4B), and we observed no such coherence-dependence in alpha power during the gap. Topographies illustrate the difference in alpha power between P1-high and P1-low coherence trials [-0.2 to 0s] before P2 onset. **B.** Occipital alpha power in the longest gap condition in the two experiments. In Experiment 2, where the event distribution was skewed towards short gap durations between the first and second pulses, participants' occipital alpha was significantly higher (indicating lower attention) than in Experiment 1 (* $p<0.05$; two-sample t-test for the difference in alpha power between occipital activity [-0.1 0s] before P2 and the baseline [-0.2 0s] before P1. Alpha power has been linked to temporal expectation encoding (Rohenkohl & Nobre, 2011), as well as being a well-known index of attentional engagement (Thut et al., 2006). Thus, this difference is interesting in light of the difference in gap durations in our two experiments, and hence temporal expectations. In particular, in those trials where no second pulse had been presented after a 0.5s gap, the probability of the second pulse yet appearing was 0.67 in Experiment 1, compared to 0.6 in Experiment 2. Although another difference between experiments was that early terminations within pulse 1 occurred more often in Experiment 2, as predicted by our model (see Fig. 4B), the probability of early terminations is unlikely to be the key influence given the above finding that alpha power during the gap was not dependent on P1 coherence (**A**). Rather than reflecting switches between engagement and disengagement at the decision level, then, it may reflect a gating function at the sensory processing level that operates independent of whether early bound-crossings have happened, yet is modulated between contexts depending on the likelihood of a second pulse still to come. The dotted box indicates the test period. In all panels, shaded areas indicate the timing of evidence pulses for the relevant gap durations. *Markers along the bottom of panel A indicate significant clusters where alpha power differed from zero (two-tailed cluster-based permutation test, $p<0.05$). In panel B, they indicate significant clusters where alpha power differed in P1-high vs. P1-low coherence trials.

Figure S10. Model comparison investigating the effect of drift rate variability at the second pulse.

In our main analysis, we initially fit a model with two different drift rates for low (d1) and high (d2) coherence pulses: **Model 1 (k = 3, b, d1, d2)**. Here, we explored whether increased temporal uncertainty about whether and when a second pulse might appear could have led to more variable attentional states before its appearance, and as a consequence more variable drift rates. To test this hypothesis, we extended the model with one additional free parameter introducing trial-by-trial variability to the drift rates applied to pulse 2: **Model 2 (k = 4: b, d_low, d_high, dvar_p2).** This model resulted in the lowest overall error as measured by G^2, but the additional complexity was not warranted according to AIC/BIC metrics.

		Free parameters				Goodness of fit		
		b	D1	D2	Dvar_P2	AIC	BIC	G^2
Exp. 1	*Model 1*	0.047	0.097	0.177		6.41	20.82	0.41
	Model 2	0.055	0.091	0.181	0.152	8.34	27.55	0.34
Exp 2	*Model 1*	0.037	0.117	0.205		6.82	22.50	0.82
	Model 2	0.039	0.122	0.211	0.237	8.59	29.36	0.59

Figure S11. Weight on choice modulations by single-trial fluctuations in neural evidence accumulation and attention markers.

In this analysis, we sought to investigate whether single-trial fluctuations in the neural correlates of evidence accumulation and attention were linked to variability in choice behaviour. To do so, we exploited the trial-by-trial variability in the neural signals. **A.** Standardized regression coefficients (±SEM) resulting from Eq. 9, illustrating the effect of CPP-P1 (*left*) and CPP-P2 (*right*) variability on choice, averaged across all gap conditions. The magnitude of CPP-P1 modulated the impact of the first pulse on choices in both experiments while the magnitude of CPP-P2 only modulated the relative weight of P2 in Experiment 2. In our task, variability in the CPP may be related to trial-by-trial variability in motion energy, as well as random noise. Since the weight on choice of P1 and P2 may trade-off with one another due to a bound being set – i.e. on trials where P1 has a strong influence, P2 is likely to have a weaker one - we also computed the difference between the two modulatory terms ([P1coh*CPP - minus P2coh*CPP], for CPP-P1 and CPP-P2 respectively). This difference index effectively quantifies whether centroparietal responses to either pulse modulate the relative weight on choice of each of the pulses. A positive index indicates a relative increase of P1 weight on choice, whereas a negative index indicates a relative increase of P2 weight on choice. Black dashed lines correspond to the difference in regression coefficients for the [P1coh*CPP – P2coh*CPP modulations]. **B.** Standardized regression coefficients (±SEM) resulting from Eq. 10 for alpha aligned to pulse 1 (*left*) or pulse 2 (*right*), averaged across all gap conditions. The magnitude of occipital phasic alpha responses (baselined before P1) did not modulate the weight on choice of P1, and after P2 did modulate its weight on choice in Experiment 2 only. Black dashed lines correspond to the difference in regression coefficients for the P1*alpha – P2*alpha modulations, which effectively indicate a change in the relative weight for P1 and P2. *Asterisks along the bottom of the panels indicate significant (p<0.05) effects in the test period [0.2-0.8s post event].

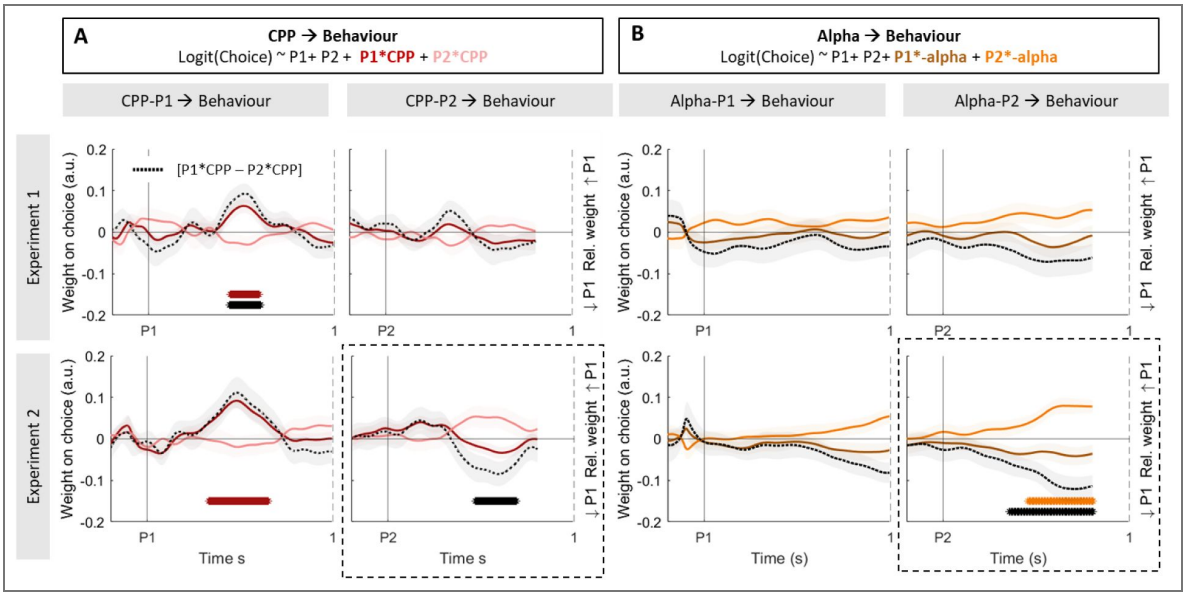

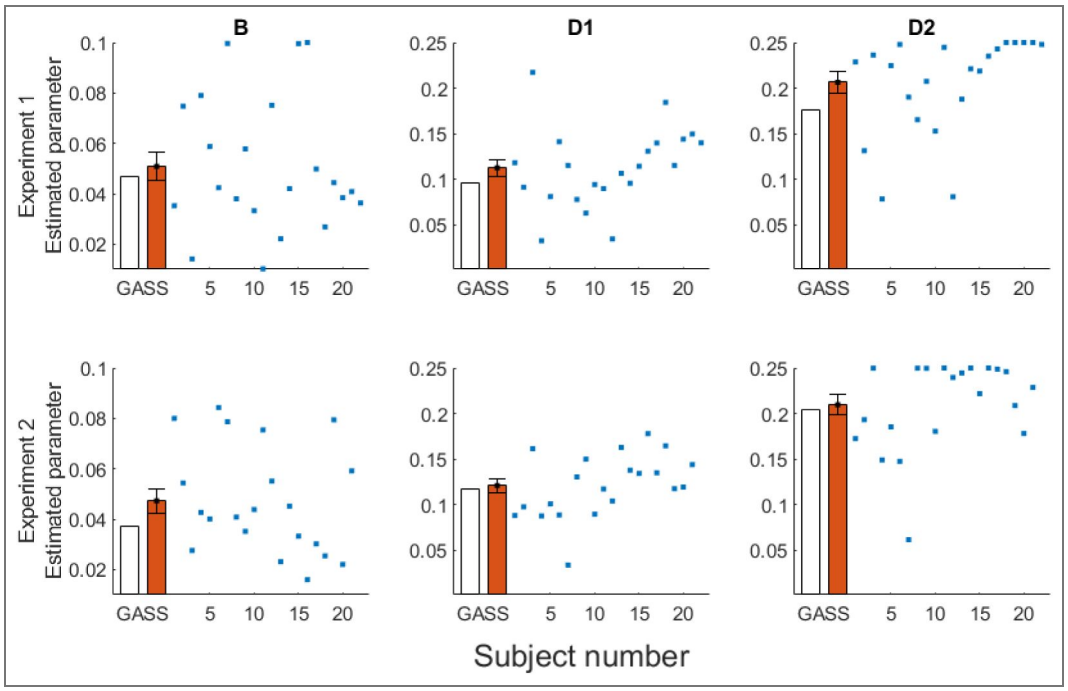

Figure S12. Model parameters (bound (B), low drift rate (D1), high drift rate (D2)) obtained using grand-averaged data (white bars) in each experiment, used for the analyses and simulations in the main manuscript.

To assess the robustness and variability of these results across participants, we additionally fit the same model to each individual participant (N = 5000, blue dots). Orange bars indicate the mean (± SEM) of these individually-estimated parameters. The averaged parameters qualitatively recapitulate the results from the model based on grand-averaged data.

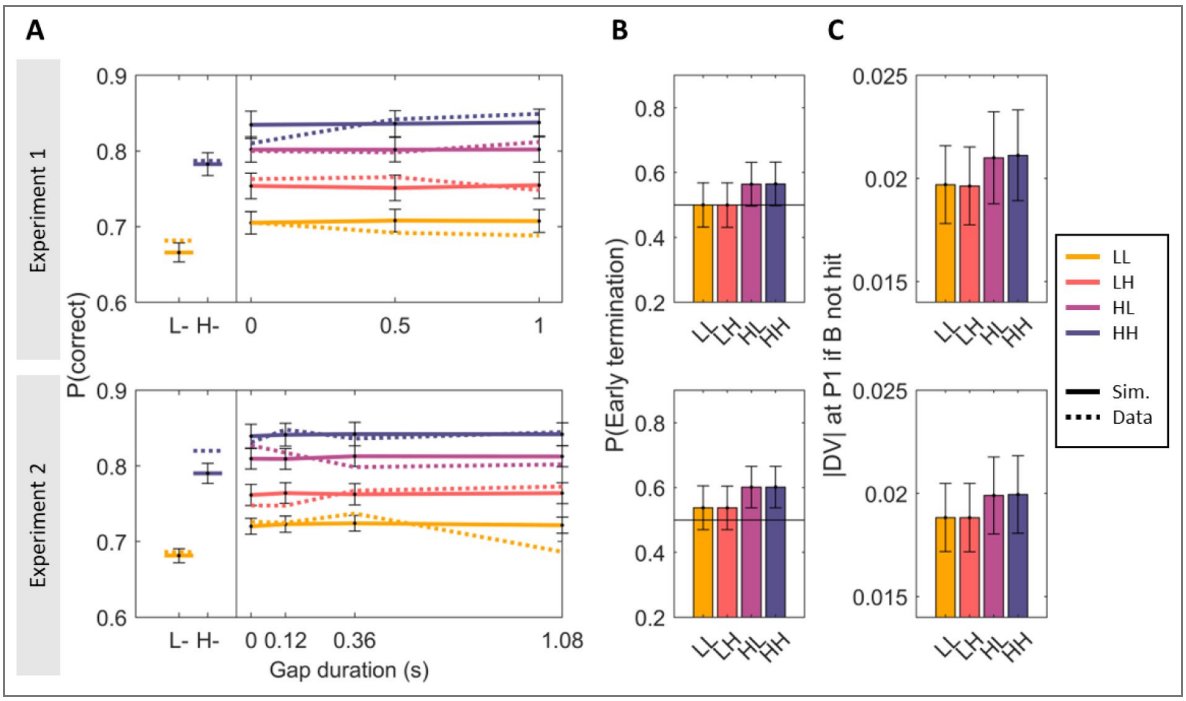

Figure S13. Replication of results in Figure 4, using models fit to individual participants rather than to the grand-averaged data.

We used the individually-fit parameters (B (bound), d1 (low drift rate), d2 (high drift rate)), to simulate N = 10000 for each participant. Data shown here represent the average of all simulations across participants, and error bars indicate the Standard Error of the Mean (SEM). These simulations of individual data fits closely match the results obtained using the model fit to the grand-averaged data. **A.** Grand-averaged simulated (*solid lines*) accuracy in single- (*left*) and two-pulse (*right*) trials, sorted by pulse coherence and gap duration in experiments 1 (*top*) and 2 (*bottom*). Observed data are overlaid (*dashed*) for comparison. **B.** Proportion (mean ± SEM) of simulated two-pulse trials that hit a bound during the first pulse, and therefore did not use the second pulse evidence to make a choice. **C.** Absolute value (mean ± SEM) of the decision variable (DV) at the end of pulse 1 in the subset of trials where the bound was not hit during that pulse, sorted by condition.

Data availability

All raw EEG and behavioural data in this study as well as analysis code are publicly available in an OSF repository: *https://osf.io/z7dp2/*

Acknowledgements

This work was supported by a grant from Science Foundation Ireland (now Taighde Éireann) under grant number 19/US/3599, an Investigator Award from the Wellcome Trust under grant number 219572/Z/19/Z (to S.P.K) and a grant from the European Research Council (ERC): Consolidator Grant 'IndDecision' under grant number 865474. The authors would also like to thank Mike Shadlen for discussions on this work, and students Liang Tong and Bowen Duan for assistance during data collection.

Additional information

Author contributions

Conceptualisation: E.P-P, & S.P.K; software: E.P-P; data curation & analysis: E.P-P.; resources: S.P.K.; writing of original draft: E.P-P.; review & editing: E.P-P, R.G.O., A.C.G, & S.P.K.; supervision: S.P.K.

Funding

Funder	Grant reference number	Author
Science Foundation Ireland (SFI)	19/US/3599	Simon P Kelly
Wellcome Trust (WT)	https://doi.org/10.35802/219572	Simon P Kelly
EC | European Research Council (ERC)	https://doi.org/10.3030/865474	Redmond G O'Connell

Author ORCID iDs

Elisabeth Parés-Pujolràs: https://orcid.org/0000-0002-2176-3299
Simon P Kelly: https://orcid.org/0000-0001-9983-3595

References

1. **Afacan-Seref K.,** Steinemann N. A., Blangero A., Kelly S. P (2018) Dynamic Interplay of Value and Sensory Information in High-Speed Decision Making. *Current Biology* **28**:795-802.e6. https://doi.org/10.1016/J.CUB.2018.01.071 | PubMed
2. **Azizi Z.,** Ebrahimpour R (2023) Explaining Integration of Evidence Separated by Temporal Gaps with Frontoparietal Circuit Models. *Neuroscience* **509**:74-95 https://doi.org/10.1016/J.NEUROSCIENCE.2022.10.019 | PubMed
3. **Balsdon T.,** Mamassian P., Wyart V (2021) Separable neural signatures of confidence during perceptual decisions. *eLife* **10** https://doi.org/10.7554/eLife.68491 | PubMed
4. **Balsdon T.,** Wyart V., Mamassian P (2020) Confidence controls perceptual evidence accumulation. *Nature Communications* **11** https://doi.org/10.1038/s41467-020-15561-w | PubMed
5. **Bates D. M** (2011) Mixed models in R using the lme4 package Part 1: Linear mixed models with simple , scalar random effects. *Analysis* https://doi.org/10.2174/1568008054863754
6. **Ben-Shachar M. S.** (2018) TBT: Reject and Interpolate channels on a trial-by-trial basis. Zenodo. https://doi.org/10.5281/zenodo.1438651
7. **Bronfman Z. Z.,** Brezis N., Usher M (2016) Non-monotonic Temporal-Weighting Indicates a Dynamically Modulated Evidence-Integration Mechanism. *PLOS Computational Biology* **12**:e1004667 https://doi.org/10.1371/JOURNAL.PCBI.1004667 | PubMed

8. **Brunner C.,** Delorme A., Makeig S., Diego S (2013) Eeglab – an Open Source Matlab Toolbox for Electrophysiological Research. *Biomed Tech* **58** https://doi.org/10.1515/bmt-2013-4182
9. **Brunton B. W.,** Botvinick M. M., Brody C. D (2013) Rats and humans can optimally accumulate evidence for decision-making. *Science* **340**:95-98 https://doi.org/10.1126/science.1233912
10. **Cheadle S.,** Wyart V., Tsetsos K., Myers N., de Gardelle V., Herce Castañón S., Summerfield C. (2014) Adaptive Gain Control during Human Perceptual Choice. *Neuron* **81**:1429-1441 https://doi.org/10.1016/j.neuron.2014.01.020 | PubMed
11. **Chung Y.,** Gelman A., Rabe-Hesketh S., Liu J., Dorie V (2015) Weakly Informative Prior for Point Estimation of Covariance Matrices in Hierarchical Models. *Journal of Educational and Behavioral Statistics* **40**:136-157 https://doi.org/10.3102/1076998615570945
12. **Chung Y.,** Rabe-Hesketh S., Dorie V., Gelman A., Liu J (2013) A Nondegenerate Penalized Likelihood Estimator for Variance Parameters in Multilevel Models. *Psychometrika* **78**:685-709 https://doi.org/10.1007/s11336-013-9328-2 | PubMed
13. **de Lange F. P.,** Rahnev D. A., Donner T. H., Lau H. (2013) Prestimulus oscillatory activity over motor cortex reflects perceptual expectations. *Journal of Neuroscience* **33**:1400-1410 https://doi.org/10.1523/JNEUROSCI.1094-12.2013 | PubMed
14. **Delorme A.,** Makeig S (2004) EEGLAB: An open source toolbox for analysis of single-trial EEG dynamics including independent component analysis. *Journal of Neuroscience Methods* **134**:9-21 https://doi.org/10.1016/j.jneumeth.2003.10.009 | PubMed
15. **Donner T. H.,** Siegel M., Fries P., Engel A. K (2009) Buildup of Choice-Predictive Activity in Human Motor Cortex during Perceptual Decision Making. *Current Biology* https://doi.org/10.1016/j.cub.2009.07.066 | PubMed
16. **Feuerriegel D.,** Jiwa M., Turner W. F., Andrejević M., Hester R., Bode S (2021) Tracking dynamic adjustments to decision making and performance monitoring processes in conflict tasks. *NeuroImage* **238**:118265 https://doi.org/10.1016/j.neuroimage.2021.118265 | PubMed
17. **Foxe J. J.,** Snyder A. C (2011) The role of alpha-band brain oscillations as a sensory suppression mechanism during selective attention. *Frontiers in Psychology* **2**:10747 https://doi.org/10.3389/fpsyg.2011.00154
18. **Geuzebroek A. C.,** Craddock H., O'Connell R. G., Kelly S. P (2023) Balancing true and false detection of intermittent sensory targets by adjusting the inputs to the evidence accumulation process. *eLife* **12** https://doi.org/10.7554/ELIFE.83025 | PubMed
19. **Gherman S.,** Markowitz N., Tostaeva G., Espinal E., Mehta A. D., O'Connell R. G., Kelly S. P., Bickel S (2024) Intracranial electroencephalography reveals effector-independent evidence accumulation dynamics in multiple human brain regions. *Nature Human Behaviour* **8**:758-770 https://doi.org/10.1038/s41562-024-01824-9 | PubMed
20. **Glickman M.,** Moran R., Usher M (2022) Evidence integration and decision confidence are modulated by stimulus consistency. *Nature Human Behaviour* **6**:988-999 https://doi.org/10.1038/s41562-022-01318-6 | PubMed
21. **Gold J. I.,** Shadlen M. N (2007) The neural basis of decision making. *Annual Review of Neuroscience* **30**:535-574 https://doi.org/10.1146/annurev.neuro.29.051605.113038 | PubMed
22. **Golmohamadian M.,** Faraji M., Fallah F., Sharifizadeh F., Ebrahimpour R (2025) Flexibility in choosing decision policies in gathering discrete evidence over time. *PLOS One* **20**:e0316320 https://doi.org/10.1371/journal.pone.0316320 | PubMed
23. **Gould I. C.,** Nobre A. C., Wyart V., Rushworth M. F. S (2012) Effects of Decision Variables and Intraparietal Stimulation on Sensorimotor Oscillatory Activity in the Human Brain. *Journal of Neuroscience* **32**:13805-13818 https://doi.org/10.1523/JNEUROSCI.2200-12.2012 | PubMed
24. **Haegens S.,** Nácher V., Hernández A., Luna R., Jensen O., Romo R (2011) Beta oscillations in the monkey sensorimotor network reflect somatosensory decision making. *Proceedings of the National Academy of Sciences* **108**:10708-10713 https://doi.org/10.1073/pnas.1107297108 | PubMed

25. **Haegens S.,** Vergara J., Rossi-Pool R., Lemus L., Romo R (2017) Beta oscillations reflect supramodal information during perceptual judgment. *Proceedings of the National Academy of Sciences* **114**:13810-13815 https://doi.org/10.1073/pnas.1714633115 | PubMed

26. **Hanks T. D.,** Summerfield C (2017) Perceptual Decision Making in Rodents, Monkeys, and Humans. *Neuron* **93**:15-31 https://doi.org/10.1016/J.NEURON.2016.12.003 | PubMed

27. **Heekeren H. R.,** Marrett S., Ungerleider L. G (2008) The neural systems that mediate human perceptual decision making. *Nature Reviews Neuroscience* **9**:467-479 https://doi.org/10.1038/nrn2374 | PubMed

28. **Herding J.,** Spitzer B., Blankenburg F (2016) Upper Beta Band Oscillations in Human Premotor Cortex Encode Subjective Choices in a Vibrotactile Comparison Task. *Journal of Cognitive Neuroscience* **28**:668-679 https://doi.org/10.1162/jocn_a_00932 | PubMed

29. **Hyafil A.,** Rocha J. de la, Pericas C., Katz L. N., Huk A. C., Pillow J. W. (2023) Temporal integration is a robust feature of perceptual decisions. *eLife* **12** https://doi.org/10.7554/ELIFE.84045 | PubMed

30. **Kayser J.,** Tenke C. E (2006) Principal components analysis of Laplacian waveforms as a generic method for identifying ERP generator patterns: I. Evaluation with auditory oddball tasks. *Clinical Neurophysiology* **117**:348-368 https://doi.org/10.1016/j.clinph.2005.08.034 | PubMed

31. **Kelly S. P.,** Corbett E. A., O'Connell R. G (2021) Neurocomputational mechanisms of prior-informed perceptual decision-making in humans. *Nature Human Behaviour* **5**:467-481 https://doi.org/10.1038/s41562-020-00967-9 | PubMed

32. **Kelly S. P.,** O'Connell R. G (2013) Internal and External Influences on the Rate of Sensory Evidence Accumulation in the Human Brain. *Journal of Neuroscience* **33**:19434-19441 https://doi.org/10.1523/jneurosci.3355-13.2013 | PubMed

33. **Keung W.,** Hagen T. A., Wilson R. C (2019) Regulation of evidence accumulation by pupil-linked arousal processes. *Nature Human Behaviour* **3**:636-645 https://doi.org/10.1038/s41562-019-0551-4 | PubMed

34. **Keung W.,** Hagen T. A., Wilson R. C (2020) A divisive model of evidence accumulation explains uneven weighting of evidence over time. *Nature Communications* **11**:2160 https://doi.org/10.1038/s41467-020-15630-0 | PubMed

35. **Kiani R.,** Churchland A. K., Shadlen M. N (2013) Integration of direction cues is invariant to the temporal gap between them. *Journal of Neuroscience* **33**:16483-16489 https://doi.org/10.1523/JNEUROSCI.2094-13.2013 | PubMed

36. **Kiani R.,** Hanks T. D., Shadlen M. N (2008) Bounded integration in parietal cortex underlies decisions even when viewing duration is dictated by the environment. *The Journal of Neuroscience : The Official Journal of the Society for Neuroscience* **28**:3017-3029 https://doi.org/10.1523/JNEUROSCI.4761-07.2008 | PubMed

37. **Lange R. D.,** Chattoraj A., Beck J. M., Yates J. L., Haefner R. M (2021) A confirmation bias in perceptual decision-making due to hierarchical approximate inference. *PLOS Computational Biology* **17**:e1009517 https://doi.org/10.1371/JOURNAL.PCBI.1009517 | PubMed

38. **Levitt H** (1971) Transformed Up-Down Methods in Psychoacoustics. *The Journal of the Acoustical Society of America* **49**:467-477 https://doi.org/10.1121/1.1912375 | PubMed

39. **Liu T.,** Pleskac T. J (2011) Neural correlates of evidence accumulation in a perceptual decision task. *Journal of Neurophysiology* **106**:2383-2398 https://doi.org/10.1152/jn.00413.2011 | PubMed

40. **Lopez-Calderon J.,** Luck S. J (2014) ERPLAB: An open-source toolbox for the analysis of event-related potentials. *Frontiers in Human Neuroscience* **8**:213 https://doi.org/10.3389/fnhum.2014.00213 | PubMed

41. **Maris E.,** Oostenveld R (2007) Nonparametric statistical testing of EEG- and MEG-data. *Journal of Neuroscience Methods* **164**:177-190 https://doi.org/10.1016/j.jneumeth.2007.03.024 | PubMed

42. **Mazurek M. E.,** Roitman J. D., Ditterich J., Shadlen M. N (2003) A Role for Neural Integrators in Perceptual Decision Making. *Cerebral Cortex* **13**:1257-1269 https://doi.org/10.1093/CERCOR/BHG097 | PubMed

43. **McCone H.,** Devine C. A., McNickle E., Dully J., Geuzebroek A. C., McGovern D. P., Kelly S. P., O'Connell R. G (2026) A Movement-Independent Signature of Urgency During Human Perceptual Decision Making. *Journal of Neuroscience* https://doi.org/10.1523/JNEUROSCI.1445-25.2025 | PubMed

44. **Murphy P. R.,** Boonstra E., Nieuwenhuis S (2016) Global gain modulation generates time-dependent urgency during perceptual choice in humans. *Nature Communications* **7**:1-14 https://doi.org/10.1038/ncomms13526 | PubMed

45. **Murphy P. R.,** Wilming N., Hernandez-Bocanegra D. C., Prat-Ortega G., Donner T. H (2021) Adaptive circuit dynamics across human cortex during evidence accumulation in changing environments. *Nature Neuroscience* **24**:987-997 https://doi.org/10.1038/s41593-021-00839-z | PubMed

46. **O'Connell R. G.,** Dockree P. M., Kelly S. P (2012) A supramodal accumulation-to-bound signal that determines perceptual decisions in humans. *Nature Neuroscience* https://doi.org/10.1038/nn.3248 | PubMed

47. **O'Connell R. G.,** Kelly S. P (2021) Neurophysiology of Human Perceptual Decision-Making. *Annual Review of Neuroscience* **44**:495-516 https://doi.org/10.1146/annurev-neuro-092019-100200 | PubMed

48. **Okazawa G.,** Kiani R (2023) Neural Mechanisms That Make Perceptual Decisions Flexible. *Annual Review of Physiology* **85**:191-215 https://doi.org/10.1146/annurev-physiol-031722-024731

49. **Oostenveld R.,** Fries P., Maris E., Schoffelen J. M (2011) FieldTrip: Open source software for advanced analysis of MEG, EEG, and invasive electrophysiological data. *Computational Intelligence and Neuroscience* https://doi.org/10.1155/2011/156869 | PubMed

50. **Pape A.-A.,** Siegel M (2016) Motor cortex activity predicts response alternation during sensorimotor decisions. *Nature Communications* **7**:13098 https://doi.org/10.1038/ncomms13098 | PubMed

51. **Parés-Pujolràs E.,** Kelly S. P., Murphy P. R (2025) Dissociable encoding of evolving beliefs and momentary belief updates in distinct neural decision signals. *Nature Communications* **16**:1-14 https://doi.org/10.1038/s41467-025-58861-9 | PubMed

52. **Pereira M.,** Megevand P., Tan M. X., Chang W., Wang S., Rezai A., Seeck M., Corniola M., Momjian S., Bernasconi F., *et al.* (2021) Evidence accumulation relates to perceptual consciousness and monitoring. *Nature Communications* **12**:3261 https://doi.org/10.1038/s41467-021-23540-y | PubMed

53. **Pfurtscheller G.,** Lopes da Silva F. H. (1999) Event-related EEG/MEG synchronization and desynchronization: Basic principles. *Clinical Neurophysiology* **110**:1842-1857 https://doi.org/10.1016/S1388-2457(99)00141-8 | PubMed

54. **Ploran E. J.,** Nelson S. M., Velanova K., Donaldson D. I., Petersen S. E., Wheeler M. E (2007) Evidence Accumulation and the Moment of Recognition: Dissociating Perceptual Recognition Processes Using fMRI. *Journal of Neuroscience* **27**:11912-11924 https://doi.org/10.1523/JNEUROSCI.3522-07.2007 | PubMed

55. **Rassi E.,** Zhang Y., Mendoza G., Méndez J. C., Merchant H., Haegens S (2023) Distinct beta frequencies reflect categorical decisions. *Nature Communications* **14**:2923 https://doi.org/10.1038/s41467-023-38675-3 | PubMed

56. **Rohenkohl G.,** Nobre A. C (2011) Alpha Oscillations Related to Anticipatory Attention Follow Temporal Expectations. *Journal of Neuroscience* **31**:14076-14084 https://doi.org/10.1523/JNEUROSCI.3387-11.2011 | PubMed

57. **Rouault M.,** Weiss A., Lee J. K., Drugowitsch J., Chambon V., Wyart V (2022) Controllability boosts neural and cognitive signatures of changes-of-mind in uncertain environments. *eLife* **11** https://doi.org/10.7554/ELIFE.75038 | PubMed

58. **Shadlen M. N.,** Kiani R (2013) Decision making as a window on cognition. *Neuron* **80**:791-806 https://doi.org/10.1016/j.neuron.2013.10.047 | PubMed

59. **Sospedra A.,** Canals S., Marcos E., Hernández M., Joan S (2025) A temporal gap in sensory streams amplifies the influence of subsequent input on decision making. *bioRxiv* https://doi.org/10.1101/2024.07.17.603868

60. **Stancák A.,** Pfurtscheller G (1995) Desynchronization and recovery of β rhythms during brisk and slow self-paced finger movements in man. *Neuroscience Letters* **196**:21-24 https://doi.org/10.1016/0304-3940(95)11827-J | PubMed

61. **Steinemann N. A.,** O'Connell R. G., Kelly S. P (2018) Decisions are expedited through multiple neural adjustments spanning the sensorimotor hierarchy. *Nature Communications* **9**:3627 https://doi.org/10.1038/s41467-018-06117-0 | PubMed

62. **Stockart F.,** Msheik R., Robin A., Jurkovičová L., Goueytes D., Rouy M., Mareček R., Hoffmann D., Mudrik L., Roman R., *et al.* (2025) Cortical evidence accumulation for visual perception occurs irrespective of reports. *Nature Communications* **16**:8458 https://doi.org/10.1038/s41467-025-63255-y | PubMed

63. **Tohidi-Moghaddam M.,** Zabbah S., Olianezhad F., Ebrahimpour R (2019) Sequence-dependent sensitivity explains the accuracy of decisions when cues are separated with a gap. *Attention. Perception, and Psychophysics* **81**:2745-2754 https://doi.org/10.3758/s13414-019-01810-8

64. **Tremel J. J.,** Wheeler M. E (2015) Content-specific evidence accumulation in inferior temporal cortex during perceptual decision-making. *NeuroImage* **109**:35-49 https://doi.org/10.1016/j.neuroimage.2014.12.072 | PubMed

65. **Tsetsos K.,** Gao J., McClelland J. L., Usher M (2012) Using time-varying evidence to test models of decision dynamics: Bounded diffusion vs. The leaky competing accumulator model. *Frontiers in Neuroscience* **6**:1-17 https://doi.org/10.3389/fnins.2012.00079 | PubMed

66. **Twomey D. M.,** Kelly S. P., O'Connell R. G (2016) Abstract and effector-selective decision signals exhibit qualitatively distinct dynamics before delayed perceptual reports. *Journal of Neuroscience* **36**:7346-7352 https://doi.org/10.1523/JNEUROSCI.4162-15.2016 | PubMed

67. **Urai A. E.,** De Gee J. W., Tsetsos K., Donner T. H. (2019) Choice history biases subsequent evidence accumulation. *eLife* **8**:1-34 https://doi.org/10.7554/eLife.46331 | PubMed

68. **Urai A. E.,** Donner T. H (2022) Persistent activity in human parietal cortex mediates perceptual choice repetition bias. *Nature Communications* **13**:6015 https://doi.org/10.1038/s41467-022-33237-5 | PubMed

69. **Van Den Brink R. L.,** Murphy P. R., Desender K., De Ru N., Nieuwenhuis S. (2021) Temporal expectation hastens decision onset but does not affect evidence quality. *Journal of Neuroscience* **41**:130-143 https://doi.org/10.1523/JNEUROSCI.1103-20.2020 | PubMed

70. **Van Diepen R. M.,** Foxe J. J., Mazaheri A. (2019) The functional role of alpha-band activity in attentional processing: The current zeitgeist and future outlook. *Current Opinion in Psychology* **29**:229-238 https://doi.org/10.1016/j.copsyc.2019.03.015 | PubMed

71. **Waskom M. L.,** Kiani R (2018) Decision Making through Integration of Sensory Evidence at Prolonged Timescales. *Current Biology* **28**:3850-3856.e9. https://doi.org/10.1016/j.cub.2018.10.021 | PubMed

72. **Wilming N.,** Murphy P. R., Meyniel F., Donner T. H (2020) Large-scale dynamics of perceptual decision information across human cortex. *Nature Communications* **11**:5109 https://doi.org/10.1038/s41467-020-18826-6 | PubMed

73. **Wyart V.,** de Gardelle V., Scholl J., Summerfield C. (2012) Rhythmic Fluctuations in Evidence Accumulation during Decision Making in the Human Brain. *Neuron* **76**:847-858 https://doi.org/10.1016/j.neuron.2012.09.015 | PubMed

74. **Wyart V.,** Myers N. E., Summerfield C (2015) Neural mechanisms of human perceptual choice under focused and divided attention. *Journal of Neuroscience* **35**:3485-3498 https://doi.org/10.1523/JNEUROSCI.3276-14.2015 | PubMed

75. **Yates J. L.,** Park I. M., Katz L. N., Pillow J. W., Huk A. C (2017) Functional dissection of signal and noise in MT and LIP during decision-making. *Nature Neuroscience* **20**:1285-1292 https://doi.org/10.1038/nn.4611 | PubMed

Parés-Pujolràs E., Kelly SP. (2026) Data from: Perceptual glimpses are locally accumulated and globally maintained at distinct processing levels. OSF. ID z7dp2 https://osf.io/z7dp2/

Peer reviews

Reviewer #1 (Public review):

Summary:

This paper characterises the physiological and computational underpinnings of the accumulation of intermittent glimpses of sensory evidence, with a focus on the centroparietal positivity and motor beta lateralization. The main finding is that the centroparietal positivity builds up during evidence accumulation but falls back to baseline during gaps, while motor beta lateralization maintains a continuous a sustained representation throughout the gap and until response.

Strengths:

- Elegant combination of electroencephalography and computational modelling.

- Innovative task design, including parametric manipulation of gap duration.

- The authors describe results of two separate experiments, with very similar results, in effect providing an internal replication.

Weaknesses:

- A direct characterization of how the centroparietal positivity and motor beta lateralization interact is missing, which limits the novelty. In their reply to reviewers, the authors argue that the signal-to-noise ratio of EEG signals is insufficient for such analyses at the single-trial level. If so, a binned or trial-averaged approach could still be attempted.

- An exhaustive characterisation of sensors and frequency bands is also missing. In their reply to reviewers, the authors suggest that this would detract from their hypothesis-driven focus. I disagree: the main hypothesis and figures could remain centred on the centroparietal positivity and motor beta lateralization, with a more comprehensive mapping of sensors and frequencies placed in supplementary material. Since the purpose of the paper is to examine EEG-based decision signals in a novel behavioural context, a broader characterisation of the underlying EEG landscape would seem appropriate.

https://doi.org/10.7554/eLife.107980.2.sa2

Reviewer #2 (Public review):

Summary:

This manuscript examines decision-making in a context where the information for the decision is not continuous, but separated by a short temporal gap. The authors use a standard motion direction discrimination task over two discrete dot motion pulses (but unlike previous experiments, fill the gaps in evidence with 0-coherence random dot motion of differently coloured dots). Previous studies using this task (Kiani et al., 2013; Tohidi-Moghaddam et al., 2019; Azizi et al., 2021; 2023) or other discrete sample stimuli (Cheadle et al., 2014; Wyart et al., 2015; Golmohamadian et al., 2025) have shown decision-makers to integrate evidence from multiple samples (although with some flexible weighting on each sample). In this experiment, decision-makers tended not to use the second motion pulse for their decision. This allows the separation of neural signatures of momentary decision-evidence samples from the accumulated decision-evidence. In this context, classic electroencephalography

signatures of accumulated decision-evidence (central-parietal positivity) are shown to reflect the momentary decision-evidence samples.

Strengths:

The authors present an excellent analysis of the data in support of their findings. In terms of proportion correct, participants show poorer performance than predicted if assuming both evidence samples were integrated perfectly. A regression analysis suggested a weaker weight on the second pulse, and in line with this, the authors show an effect of the order of pulse strength that is reversed compared to previous studies: A stronger second pulse resulted in worse performance than a stronger first pulse (this is in line with the visual condition reported in Golmohamadian et al., 2025). The authors also show smaller changes in electrophysiological signatures of decision-making (central parietal positivity, and lateralised motor beta power) in response to the second pulse. The authors describe these findings with a computational model which allows for early decision-commitment, meaning the second pulse is ignored on the majority of trials. The model-predicted electrophysiological components describe the data well. In particular, this analysis of model-predicted electrophysiology is impressive in providing simple and clear predictions for understanding the data.

Weaknesses:

Some readers may be left questioning why behaviour in this experiment is so different from previous experiments which use almost exactly the same design (Kiani et al., 2013; Tohidi-Moghaddam et al., 2019; Azizi et al., 2021; 2023). Overall performance in this experiment was much worse than previous experiments: Participants achieved ~85% correct following 400 ms of 33 - 45% coherent motion. In previous work, performance was ~90% correct following 240ms of 12.8% coherent motion. A second weakness is that, while the authors present a model which describes the data based on pre-mature decision-commitment, they do not examine explanations from the existing literature, that evidence is flexibly weighted, and do not provide any analyses which could be used to compare these descriptions. While their model can describe the data in this manuscript, it cannot explain the data from previous experiments showing a stronger weight on the second pulse.

https://doi.org/10.7554/eLife.107980.2.sa1

Author response:

The following is the authors' response to the original reviews.

> ***Public Reviews:***
>
> ***Reviewer #1 (Public review):***
>
> *Summary:*
>
> *This paper aims to characterise the physiological and computational underpinnings of the accumulation of intermittent glimpses of sensory evidence.*
>
> *Strengths:*
>
> *(1) Elegant combination of electroencephalography and computational modelling.*
>
> *(2) The authors describe results of two separate experiments, with very similar results, in effect providing an internal replication.*
>
> *(3) Innovative task design, including different gap durations.*

> *Weaknesses:*
>
> *(1) The authors introduce the CPP as tracking an intermediary (motor-independent) evidence integration process, and the MBL as motor preparation that maintains a sustained representation of the decision variable. It would help if the authors could more directly and quantitatively assess whether their current data are in line with this. That is, do these signals exhibit key features of evidence accumulation (slope proportional to evidence strength, terminating at a common amplitude that reflects the bound)? Additionally, plotting these signals report locked (to the button press) would help here. What do the results mean for the narrative of this paper?*

The reviewer is correct that properties such as temporal slope scaling with evidence strength and stereotyped threshold-like amplitude were key in establishing that the CPP reflects evidence accumulation in conventional continuous-stimulus tasks, and its motor independence was demonstrated in how it exhibited the same evidence-dependent dynamics in the absence of motor requirements (e.g. O'Connell et al 2012). We agree that it is of interest to check any such properties that can be feasibly tested in the current, distinct task context of intermittent evidence with delayed responses. Given the way in which participants performed our delayed-response task, sometimes terminating decisions early, it is in the CPP-P1 that conventional patterns of coherence-dependence in slope and amplitude would be expected. Indeed, we found that the CPP-P1 reached higher amplitudes (Fig. 3A, Author response image 1) and exhibited a steeper build up in high- compared to low-coherence trials (Author response image 1). The slope and amplitude profile of the CPP-P2 is complex due to the variability in baseline activity across our various delay conditions and the bounded process that participants engaged in, but it is still consistent with an accumulation process. Our simulations provide a full account of how an accumulating signal could produce the observed results.

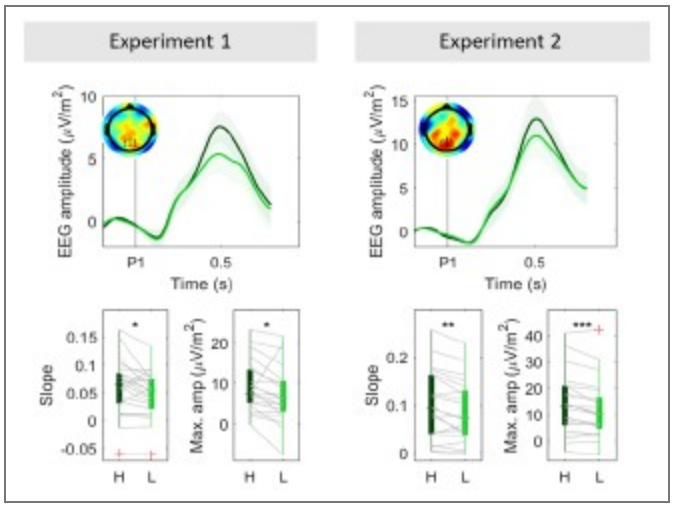

Author response image 1. Grand-averaged (± sem) CPP-P1 traces in both experiments (top). Bottom boxplot graphs indicate the average slope computed as the slope between 0.2 s post P1 onset (when CPP begins its buildup) and the time when peak amplitude was reached within the [0.4-0.6s] interval, computed for each subject individually. Red crosses indicate outliers, computed as values exceeding 1.5 times the interquartile range away from the bottom or top of the box. Grey lines indicate single subject estimates, and asterisks reflect the significance of paired ttests for the estimated slope and amplitude effects; **p<0.01, *p<0.05. H = high coherence, L = low coherence.

Like in other delayed-response tasks (Twomey et al 2016; McCone et al 2026), we observe here that the CPP peaks and falls well before the response is cued or indeed executed (here, in fact

peaking and falling for each individual pulse). Thus, its pre-response dynamics will not relate to stimulus-driven evidence accumulation in the way they do in immediate response contexts (e.g. O'Connell et al. 2012; Steinemann et al. 2018). We therefore do not analyse response-aligned CPPs in the experiment.

As to the intermediary role we have interpreted for the CPP, in addition to the local pulse driven peak-and-fall dynamics compared to the sustained profiles of motor preparation signals, we can point to the obvious temporal delay between the signals, where evidence-dependent buildup in the CPP substantially precedes that of motor preparation, as observed in all previous studies comparing the two (e.g. Kelly & O'Connell 2013).

> *(2) The novelty of this work lies partly in the aim to characterize how the CPP and MBL interact (page 5, line 3-5). However, this analysis seems to be missing. E.g., at the single-trial level, do relatively strong CPP pulses predict faster/larger MBL? The simulations in Figure 5 are interesting, but more could be done with the measured physiology.*

As exemplified in the extant EEG-decision literature, the low signal-to-noise ratio of EEG is such that attempts are seldom made to link two EEG signals on a single-trial basis, and studies instead favour testing single-trial relationships between each individual EEG signal and behaviour, or, most commonly, comparing patterns of variation in the EEG signals across experimental conditions (e.g. difficulty). Accordingly, here we show that trials with high coherence P1 evoked 1) higher CPP amplitudes (Fig. 3A,C), and 2) stronger MBL (Fig. S2 & S3). Further, we showed that particularly high CPP amplitudes following the first pulse led to stronger weights on choice for the first pulse (Fig. S11), which could only be mediated by the motor system.

> *(3) The focus on CPP and MBL is hypothesis-driven but also narrow. Since we know only a little about the physiology during this "gaps" task, have the authors considered computing TFRs from different sensor groupings (perhaps in a supplementary figure?).*

While we agree that it might be interesting to explore frequency bands and sensors more broadly, we feel that such an exploration would detract from the hypothesis-driven focus on how prominent, well-characterised decision signals in the brain behave in a context where evidence is presented in an atypical, seldom-studied manner, namely in the form of temporally separate pulses. Our aim was not to explore whole-brain dynamics that might be engaged during the task, but rather to get a better understanding of the functional roles of the neural processes underlying the CPP and MBL during decision making. Providing a detailed description of whole-scalp responses is thus beyond the scope of this paper, but given that all data will be made publicly available this can be pursued in future work and by other researchers.

> *(4) The idea of a potential bound crossing during P1 is elegant, albeit a little simplistic. I wonder if the authors could more directly show a physiological signature of this. For example, by focusing on the MBL or occipital alpha split by the LL, LH, HL and HH conditions, and showing this pulse- as well as report-locked. Related, a primacy effect can also be achieved by modelling (i) self-excitation of the current one-dimensional accumulator, or (ii) two competing accumulators that produce winner-take-all dynamics. Is it possible to distinguish between these models, either with formal model comparison or with diagnostic physiological signatures?*

In addition to the CPP amplitude effects we report in the main paper, the reviewer is correct that pulse-locked MBL can also provide a physiological signature of the greater number of pulse-1 bound crossings when that pulse is high-coherence. This is shown in Figure S3, where we see this coherence-dependent effect consistently across all gap durations and both experiments. Figure S2 also shows that the MBL step-change after P2 is greater in P1-low coherence trials in Experiment 1, as predicted by the bound-crossing account, and consistent

with the CPP findings. We note that this effect appears absent in Experiment 2, but this is likely because the greater proportion of shorter gap durations (0, .12, .36s) mean that updates following P2 are likely to still capture P1-driven changes, due to signal-transmission delays. Please also note that Fig. S2 and S3 have been updated from the previous version, because while revising the paper we noticed a mistake whereby we were plotting alpha band power (813Hz) rather than the intended beta (13-30Hz). The results remain qualitatively unchanged. Although there isn't sufficient single-trial signal-to-noise ratio to be able to categorise individual trials as having crossed a threshold or not, this is strong evidence in support of the coherence dependent amplitudes of the CPP and motor updates. Analyzing beta locked to the report would not be informative in this case because of the delayed reporting structure of the task and the threshold-crossing relationship beta exhibits with response execution (O'Connell et al. 2012). That is, beta will reach the same amplitude immediately prior to the response regardless of whether or not decisions were terminated during P1. Instead, we believe that the empirical CPP-P2 traces we show provide direct evidence that the second pulse was not fully integrated in all trials, and as our modelling confirms, this is consistent with bound crossings occurring sometimes before P2. First, the fact that CPP-P2 amplitudes were overall lower than CPP-P1 amplitudes mirrors the behavioural observation that the first pulse had a stronger weight on choice than the second one. Second, we show that trials where the CPP was particularly high after the first pulse were also trials where P1 also exerted a particularly strong influence on choice (see Fig. S11), further validating the idea that higher CPP amplitudes are directly related to behaviour.

Regarding self-excitation (SE) and winner-take-all competition (WTAC), these could indeed contribute to the behavioural primacy effects, but they would not detract from our central finding that the CPP does not encode a sustained representation of a decision variable, but rather reflects two rounds of evidence accumulation feeding into a single decision process. Further, it is not immediately clear whether/how these alternative models might also account for the CPP-P1/CPP-P2 results as simply as our bounded model does. While it might be theoretically possible for SE/WTAC models to explain 1) why the CPP-P2 is generally lower than the CPP-P1 across conditions, and 2) why the maximum CPP-P2 amplitudes in P1-high trials are smaller than in P1-low trials, these patterns of results are not an immediate consequence of standard implementations. Further, while the question of whether the accumulation process is perfect integration or involves SE or WTAC is certainly of additional interest, given that this is a delayed response task and does not provide information on termination timing through RT distributions, arbitrating between these modes of integration would not be straightforward with the current data.

> *(5) The way the authors specify the random effects of the structure of their mixed linear models should be specified in more detail. Now, they write: "Where possible, we included all main effects of interest as random effects to control for interindividual variability." This sounds as if they started with a model with a full random effect structure and dropped random components when the model would not converge. This might not be sufficiently principled, as random components could be dropped in many different orders and would affect the results. Do all main results hold when using classical random effects statistics on subject-wise regression coefficients?*

The equations in the paper include the full details of the random effects structure we used for each model. We note that only two of our four equations did not include a full random effect structure, indeed due to convergence issues. We have now fit these models with a maximal random effects structure (i.e. including all fixed effects as random effects as well) with the 'bobyqa' optimiser. This resulted in singular fits for both Eq. 2 (Exp. 1 and Exp. 2) and Eq. 3 (Exp. 2 only). Following previous suggestions, we used a weakly informative wishart prior (Chung et al. 2015) to regularise the random effects covariance matrix using the blme package (Chung et al. 2013), which resolved the singular fit problem. However, the model still produced convergence warnings in some models. To assess these models' robustness, we

compared the fixed effect parameter estimates across multiple optimisers, as suggested by the lme4 developers (see lm4 documentation). Parameter estimates across optimisers rarely deviated by more than one decimal point across 6 optimisers (see Bates et al. 2011), and we thus concluded the model estimates were robust and convergence warnings were a false positive, a known issue in lme4. For all models in the paper, we report the parameters estimated using the "bobyqa" optimiser. All main inferential results remain unchanged (except for one interaction that was not of interest in Exp. 1), and the estimated slopes and statistical results for all models have been updated in the manuscript. We also included all these details in the manuscript.

> ***Reviewer #2 (Public review):***
>
> *Summary:*
>
> *This manuscript examines decision-making in a context where the information for the decision is not continuous, but separated by a short temporal gap. The authors use a standard motion direction discrimination task over two discrete dot motion pulses (but unlike previous experiments, fill the gaps in evidence with 0-coherence random dot motion of differently coloured dots). Previous studies using this task (Kiani et al., 2013; Tohidi-Moghaddam et al., 2019; Azizi et al., 2021; 2023) or other discrete sample stimuli (Cheadle et al., 2014; Wyart et al., 2015; Golmohamadian et al., 2025) have shown decision-makers to integrate evidence from multiple samples (although with some flexible weighting on each sample). In this experiment, decision-makers tended not to use the second motion pulse for their decision. This allows the separation of neural signatures of momentary decision-evidence samples from the accumulated decision-evidence. In this context, classic electroencephalography signatures of accumulated decision-evidence (central-parietal positivity) are shown to reflect the momentary decision-evidence samples.*
>
> *Strengths:*
>
> *The authors present an excellent analysis of the data in support of their findings. In terms of proportion correct, participants show poorer performance than predicted if assuming both evidence samples were integrated perfectly. A regression analysis suggested a weaker weight on the second pulse, and in line with this, the authors show an effect of the order of pulse strength that is reversed compared to previous studies: A stronger second pulse resulted in worse performance than a stronger first pulse (this is in line with the visual condition reported in Golmohamadian et al., 2025). The authors also show smaller changes in electrophysiological signatures of decision-making (central parietal positivity and lateralised motor beta power) in response to the second pulse. The authors describe these findings with a computational model which allows for early decision-commitment, meaning the second pulse is ignored on the majority of trials. The model-predicted electrophysiological components describe the data well. In particular, this analysis of model-predicted electrophysiology is impressive in providing simple and clear predictions for understanding the data.*
>
> *Weaknesses:*
>
> *Some readers may be left questioning why behaviour in this experiment is so different from previous experiments, which use almost exactly the same design (Kiani et al., 2013; TohidiMoghaddam et al., 2019; Azizi et al., 2021; 2023). The authors suggest this may be due to the staircase procedure used to calibrate the coherence of (single-pulse) dot motion stimuli for individuals at the start of the experiment. But it remains unclear why overall performance in this experiment is so bad. Participants achieved ~85% correct following 400 ms of 33 - 45% coherent motion. In previous work, performance was ~90% correct following 240ms of 12.8% coherent motion. It seems odd that adding the 0% coherent motion in the temporal gaps would impair performance so greatly, given it was*

> *clearly colour-coded. There is a lack of detail about the stimulus presentation parameters to understand whether visual processing explains the declined performance, or if there is a more cognitive/motivational explanation.*

We thank the reviewer for highlighting this. We apologise for not providing full details about the visual display, which we have included now.

The moving dots were presented centrally on the monitor, at a 5 degree aperture, and moving at a speed of 5 degrees/second. The monitor refresh rate was 60Hz for 19 participants and 85Hz for 3 participants in Experiment 1, while it was 85Hz for 19 participants and 60Hz for 2 participants in Experiment 2. Dot density in our task was similar to previous studies (16.7 dots/degree/s^2, as in Kiani & Shadlen 2013; Tohidi-Moghaddam et al. 2019; Azizi et al. 2021, 2023). However, in contrast to previous studies, we did not include any feedback on a trial-bytrial basis, instead only providing feedback at the end of each block indicating the average accuracy. This would have made it harder for participants to continually assess how well they were performing and to adjust their strategies (e.g. increase their bound for better accuracy) accordingly. We agree that the inclusion of 0% coherence dots during the gap between pulses is unlikely to have caused the participants' relatively low overall performance, especially since we did not find accuracy to be overall lower for longer 0%-coherence gaps.

Further, as the reviewer notes, we used a staircasing procedure at the beginning of the experiment which used only single pulses of evidence. This may have encouraged participants to set a bound that can usually be reached by one pulse, and the resultant early terminations meant that they seldom used the full 400ms of evidence that were available to them. In fact, we would like to thank the reviewer for pointing out Golmohamadian et al., 2025, which used a similar variable delays task structure but with different visual stimuli. They, like us, trained on a single-pulse task version and omitted trial-by-trial feedback in the main task, and, also like us, reported a stronger choice reliance on pulse-1. This suggests that these two factors may suffice to induce a primacy rather than a recency effect.

There are other reasons why performance may have been different in our task compared to previous studies. For example, our task included a lead-in period that was longer than in previous studies and contained 0%-coherence dots, in order to minimise interfering VEP components (the lead in period was between 700 to 1050ms in our study, compared to 200–500 ms in Kiani & Shadlen 2013; Tohidi-Moghaddam et al. 2019 & Azizi et al. 2023, and 400 -1000 ms in Azizi & Ebrahimpour 2021). This longer and visually explicit preparation period may have acted as a warning cue, allowing participants to fully prepare before the first pulse, and again making it easier for them to hit a bound with only that information.

We have added a more detailed discussion about how our stimuli and the task characteristics may have resulted in a substantially different performance in our task compared to previous studies in the discussion section.

> ***Recommendations for the authors:***
>
> ***Reviewing Editor:***
>
> *Please consider the following reviewer suggestions for how to strengthen the evidence for your central claims, which could translate into an improved assessment of the "strength of evidence".*
>
> *Apart from these useful suggestions, I had some concerns about scholarship, because the list of studies currently cited in your introduction is exclusively from your group, while one of the phenomena of interest - motor beta power lateralization (MBL) in decision-making - has been widely studied by several groups, using also other techniques.*
>
> *I was wondering why you chose not to cite the ample MEG evidence for the role of MBL in decision-making. This has been shown both in classical random dot motion tasks (Donner et al, Curr Biol, 2009; de Lange et al, J Neurosci, 2013; Pape et al, Nat Commun,*

> *2016; Urai et al, Nat Commun, 2022) as well as in tasks involving discrete evidence samples (Wilming et al, Nat Commun, 2020; Murphy et al, Nat Neurosci, 2021). Another relevant EEG study is by Ian Gould et al, J Neurosci, 2010. There is also quite a bit of monkey LFP work (mainly by Saskia Haegens) on choice-selective beta power in the motor system of the macaque, although the link to the lateralized beta power suppression in your work and the above human E/MEG studies remains a bit elusive. I feel it would be important to provide a more balanced reflection of the existing literature on this phenomenon.*

We thank the editor for this fair comment, and we apologise for having provided a too narrow, EEG-centric view of the literature, arising from our interest in the CPP component which hasn't yet been characterised in MEG or LFPs. We have now substantially expanded the introduction to provide a more balanced and comprehensive overview of the literature.

> ***Reviewer #1 (Recommendations for the authors):***
>
> *(1) The diffusion model needs to be explained in more detail. For example, it should be explicitly stated that the model was fit to only choices, as most readers would expect reaction times. Further, it needs to be started if the model was fit separately for each subject or in one go to the group-level data. If the former, it is important to add error bars of the betweensubjects variability (in simulated and empirical data) to Figure 4A. If the latter, it would be important to determine uncertainty using bootstrapping.*

The original model was fit to grand-average data, as stated in the methods section. To assess between-subjects variability, we have re-fitted the model to each individual subject, for each experiment. The average of the individually-estimated model parameters closely recapitulated the values obtained from the fit to grand-averaged data (Fig. S12). We then simulated N = 10000 trials for each individual, and we report the grand-averaged results with error bars indicating the standard error of the mean as a supplementary figure (Fig. S13). The results replicate the ones reported in the main manuscript. We have also made it explicit that the models are fit to accuracy data but not RT.

> *(2) The authors write numerous times that the MBL exhibits an "evidence-dependent" buildup. However, should this not be "choice-dependent"? In Figure 2A, one can clearly see that the sign of MBL follows choice and not objective evidence.*

We thank the reviewer for this comment. By evidence-dependent, we mean that lateralisation towards the correct response is strongest in high-coherence trials (see Fig. S2, S3). This is indeed because the sign of MBL is choice-dependent, and participants are less likely to make mistakes in high-coherence trials. We have added a clarification sentence in the text.

> *(3) It would aid readability to add sub-conclusions at the end of each Results section.*

We have added clarifications where needed.

> *(4) In Figure 1B, I cannot see a dashed line for the HL condition. I understand that it must lie under the LH condition, but it would be good to show it separately.*

We thank the reviewer for this comment. Since we cannot show both lines separately without additional panels, given the HL and LH lines perfectly overlap, we indicate at the end of the caption that this is the case as follows: "Note that a perfect accumulator predicts identical accuracies for the HL and LH conditions, and therefore the two lines overlap."

> *(5) In Figure 4B, is the horizontal dashed line important? It is confusing because the legend incorrectly states that this is "data".*

Thanks for this observation - it was only there to indicate a 50% as a benchmark to assess how frequent early terminations are, but we agree that it was unnecessary and potentially confusing, so we have removed it from the plot.

> ***Reviewer #2 (Recommendations for the authors):***

> *(1) The authors should more directly address how behaviour in their task differs quite substantially from previous experiments with very similar designs (including why such high coherence levels are required, over a longer duration, to reach overall worse performance). Some readers may also be interested in a broader discussion of how decision-makers may use flexible weights when integrating evidence across samples over time. While the explanation of bounded accumulation is convincing in this context, Tsetsos et al., (2012) suggest recency effects (as in Cheadle et al., 2014; Wyart et al., 2015) cannot be explained by bounded accumulation, but rather integration leak. Other factors may include stimulus consistency (Glickman et al., 2022) or even choice consistency across decisions (Bronfman et all., 2015). Golmohamadian et al., 2025 demonstrated flexibility in decision strategies across sensory modalities.*

As we described above, we have added some more detailed explanation about why it might be the case that behaviour in our study differs from previous reports using similar tasks. We agree that the reversed pulse-reliance in our study compared to others presents an opportunity to discuss flexibility in decision strategy and so we have now added a broader discussion on different patterns of integration in various task contexts. We thank the reviewer for pointing out Golmohamadian et al., 2025, as they, like us, trained on a single-pulse task version and omitted trial-by-trial feedback in the main task, and, like us, reported a stronger choice reliance on pulse-1.

> *(2) Another open question is how central parietal positivity reflects an accumulation signal in the case of continuous evidence, but reflects momentary evidence in the case of discrete evidence samples. If, in both cases, the parietal evidence is passed along to motor processes for bounded decision commitment, how do motor processes deal with the changes in what is represented? Can the relationship between MBL and CPP in the model-simulated data shed some light on this? Specifically, how is the 0-gap condition treated in this simulation (which shows only 1 CPP peak but with a longer time to decay) compared to non-zero gap conditions (which show 2 peaks)?*

This is a very interesting and important point, and we thank the reviewer for raising it. We believe that the CPP in our intermittent-dots task reflects dot-motion evidence integration in the same way as in conventional continuous evidence tasks, building at an evidence dependent rate (see Author response image 1), with the only difference being that integration processes can be turned “on” or “off” depending on whether evidence is present, and can thus be temporally split into multiple “rounds” of accumulation when there is a gap.

Our model simulations assume that evidence integration is triggered by the dots turning yellow, indicating the presence of evidence, and feeds continuously to the motor system in these periods. However, it is switched off either when 1) a bound has been hit, or 2) the dots turn blue again, at which point the CPP falls (see various rates of signal decay in Fig. S7). The reason the CPP continues longer before it peaks and falls in the zero-gap condition, by this account, is because there is no dot-colour change at the end of pulse-1 to switch it off, and thus the accumulation process continues until either a bound is hit, or the yellow dots turn blue after pulse-2. When there is a non-zero gap, despite the CPP being switched off, the decision variable itself remains encoded at the motor level so that no information is lost. This requires that the same instruction that turns-off the CPP must also break or pause the flow from the CPP to the motor level and allow it to hold its current level until either a second pulse resumes a feed from a newly-triggered CPP, or response execution is cued. Thus, in our account, the accumulation process underlying the CPP in our intermittent-evidence task is identical to conventional continuous-evidence tasks, but since it can be turned “on” and “off” as a function of whether or not evidence is clearly present or absent, produces two “rounds” of integration in non-zero gap conditions. The motor process also receives a feed from the CPP as in conventional continuous-evidence tasks, but with this feed similarly gated by the presence of evidence.

A slightly different and perhaps more challenging question (which the reviewer was perhaps alluding to) relates to tasks where evidence comes not in short noisy snippets, but rather as static tokens (e.g. Wyart et al. 2012, 2015; Murphy et al. 2021; Parés-Pujolràs et al. 2025). In these instances, the CPP exhibits transient evoked responses to each token, which scale with the belief updates resulting from it (Parés-Pujolràs et al. 2025). However, it remains unclear whether these transient potentials reflect a temporally-evolving integration process to compute the appropriate belief update afforded by that token in the context of a particular task, or rather reflect the output of such a process. The former account would be similar to our interpretation of the transient deflections observed in this gaps task, which we believe capture the same temporal integration processes as those commonly observed in conventional continuous noisy stimuli paradigms, only short-lived. The latter account would instead be specific to low-noise stimuli like tokens, where the computations required for belief updating may not require a temporally-extended integration process, but rely on different mechanisms to compute belief updates (e.g. prior-based modulations of sensory encoding, attention or neural gain). These questions remain open for future investigation.

> *(3) From what I understand, the model suggests all-or-none integration of the second pulse: either the bound has not been reached and the pulse is perfectly integrated, or the bound has been reached and so the pulse is not integrated. The CPP amplitude at pulse 2 is therefore determined not only by the strength of the evidence at pulse 2 but also by the proportion of trials where the evidence is not ignored: CPP at pulse 2 is of lower amplitude because it is calculated as an average across trials where it is either similar to CPP at pulse 1 or otherwise completely absent. Another explanation for the lower average amplitude is that all trials have a smaller amplitude (somewhat different from the main conclusions of the paper). It would be nice to show the dichotomy predicted by the model in the empirical data. I'm thinking of something similar to this 'bifurcation' analysis from Sergent et al., 2021. Or more simply, estimates of CPP amplitude from single trials (perhaps an average over a short window around the peak) should be more variable at pulse 2, with some reaching similar amplitudes to pulse 1, and many close to baseline, whereas at pulse 1, there should be a more uniform cluster of amplitudes. If all CPP peak amplitudes were lower, would this motivate a model comparison where, for example, additional evidence from the second pulse was down-weighted according to certainty following the first pulse (leading to all trials down-weighting the second pulse)? This could link in nicely with some of the more nuanced analyses related to attention in the supplementary figures.*

We thank the reviewer for this insightful comment, which will help us clarify how our model works. The integration of the second pulse does not work in an all-or-none manner. In our model, the accumulation stops whenever a bound is reached at the downstream motor level. This can happen 1) at some point during the 1st pulse (no integration of pulse 2 at all), 2) during the 2nd pulse (partial integration of pulse 2, until the bound is hit), or 3) not crossed at all (full integration of pulse 2). Our model thus allows for partial integration of the second pulse rather than all-or-none. Author response image 2 shows 3 example trials that illustrate how the model works. The CPP amplitudes at pulse 2 are thus determined by two main factors: 1) whether or not accumulation of P2 is precluded by an earlier bound crossing in P1 (if it is, the CPP amplitude is assumed to equal 0), and 2) whether and when accumulation ended if it did take place. Our interpretation is that, given that trials where pulse 1 was low coherence were 1) less likely to terminate early (Fig. 4B) and 2) had achieved lower levels of accumulated evidence (Fig. 4C), the LL and LH conditions are linked to a higher proportion of trials where accumulation at pulse 2 does occur, and it lasts for a longer amount of time because the distance required to reach a bound is longer than in their pulse 1 high-coherence counterparts. We have clarified this point in the results section describing the model.

The reviewer notes: “Another explanation for the lower average amplitude is that all trials have a smaller amplitude (somewhat different from the main conclusions of the paper)”.

However, our interpretation in fact predicts that the vast majority of trials should indeed exhibit smaller amplitudes. That can again be explained by the three trial types mentioned above. Unlike in CPP-P1, there would be a majority of trials where integration does not occur at all. Only trials where evidence was at least partially integrated during P2 would be predicted to have CPPP2 amplitudes that are overall positive, and even in those instances, average amplitudes would be overall lower than CPP-P1 in trials that terminated early, because of the lower distance remaining to be covered before hitting a bound. Author response image 2 illustrates this point. Thus, the prediction regarding how CPP amplitude variance or distribution shape would compare between P1 and P2 is less straightforward than if it were all-or-none on P2, not to mention the fact that EEG noise would likely drown-out distributional features like this. We therefore focus on a comparison of the means, for which our model has the clear prediction that most trials should exhibit lower CPP-P2 amplitudes. To assess whether empirical observations meet this prediction, and following the reviewer's suggestion, we extracted the mean amplitudes around 0.45-0.55s after P1 and P2, for each single trial. CPP-P2 data were baselined using the amplitude 100 ms before P2 onset, as in Fig. S5 - note that this is likely to introduce spurious drifts due to overlapping potentials from P1, but given that grand averaged traces still qualitatively captured the key effects we assume it is a valid approach. We then pooled CPP-P1 and CPP-P2 amplitudes across pulses, and z-scored them for each participant separately. In both experiments, in a majority of participants (Exp. 1: 16/22, Exp. 2: 17/21) the median z-CPP-P1 amplitude was higher than that of z-CPP-P2. Author response image 3 illustrates the pooled distributions.

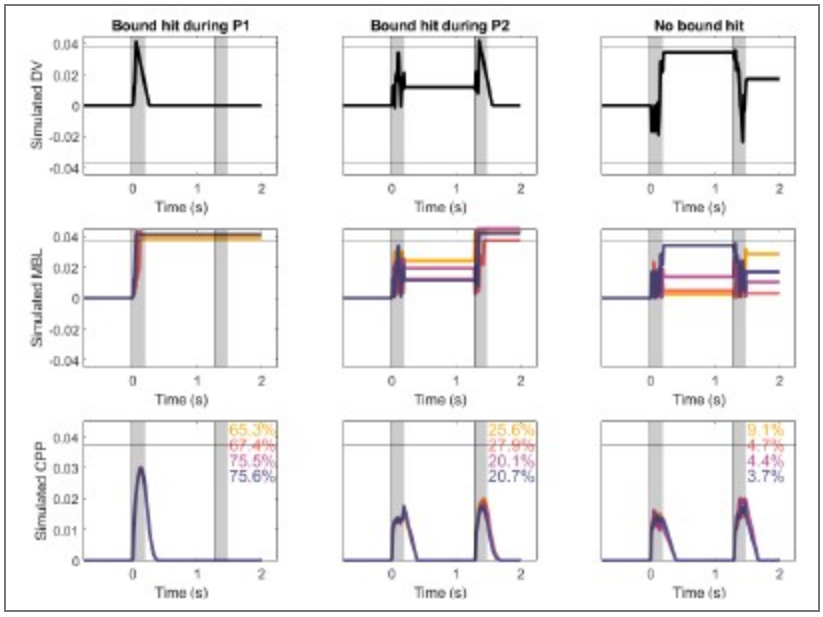

Author response image 2. Decision variable simulations illustrating sample single trials (top) and CPP traces averaging data across conditions and N = 1000 trials (bottom), using model fits from Exp 2, in the long gap condition. Overlaid text indicates the percentage of trials in each subset, for each condition. The horizontal line indicates the bound; shaded areas indicate pulse presentation times. A. The bound was hit during P1, and therefore no further accumulation occurred during P2. B. The bound was hit during P2, and therefore P2 was only partially accumulated, C. No bound was hit, and therefore all evidence from P2 was accumulated.

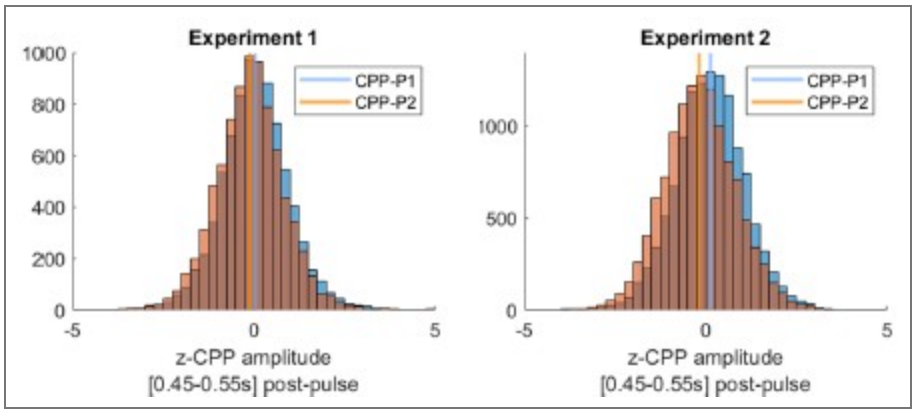

Author response image 3. Pooled CPP–P1 and CPP-P2 amplitudes [450-550ms post-pulse] distributions, normalised within-participant, and baselined 100ms before pulse onset. In both experiments, CPP-P2 amplitudes had a lower median (vertical line) normalised amplitude than CPP-P1.

> *(4) A minor note: Full details of stimulus presentation (size, number of dots, dot size, speed, lifetime) would be appreciated.*

Thank you - we have now provided these details in the methods section (see also reply to public reviews above).

> *(5) Are the authors sure they want to use this 'Gaps task' name? It seems a bit strange to introduce this name in this context, where there isn't really a 'Gap' (random dot motion fills the gap). A reader could get the impression the name was given in the Kiani et al., 2013 study (page 3, paragraph 1: "This scenario has begun to be studied using an intermittent- evidence or "gaps" task (Kiani et al., 2013) ...") but this is not true, Kiani et al. never use the term "Gaps task", nor has any other study since (as far as I know).*

We thank the reviewer for noting this oversight on our part - we have now made it clear that “gaps task” is the way we refer to the task originally developed by Kiani et al. 2013 in the introduction. We have decided to still use this name because it is a convenient proxy, in the understanding that “gap” refers to a “gap” in coherent motion as in Kiani et al (2013), albeit not a proper blank as in the original implementation.

https://doi.org/10.7554/eLife.107980.2.sa0